



Kinetic analysis of thermochemical processes for dried cattle dung

Tejas Ramaniklal Tankaria

Thesis to obtain the Master of Science Degree in

Energy Engineering and Management

Supervisor: Prof. Francisco Lemos (IST)

Dr. Adam Klimanek (SUT)

Examination Committee

Chairperson: Prof Fatima Montemor

Supervisor: Prof. Francisco Lemos

Member of the committee: Prof. João Bordado

September 2016

ॐ सहना ववतु, सहनौ भुनक्तु, सहविर्यम् करवावहे ।
तेजस्विना वधीतम् अस्तु , मा विद विशावहै ॥
ॐ शांति शांति शांति:

May He protect both of us. May He nourish both of us. May we both acquire the capacity (to study and understand the scriptures). May our study be brilliant. May we not argue with each other. Om peace, peace, peace.

Table of Contents

Acknowledgement.....	5
Abstract	6
Resumo	7
List of figures	9
List of tables	11
Chapter 1. Introduction.....	12
1.1 Types of Biomass:.....	12
1.2 Structure of Biomass.....	13
1.3 Structure of Lignocellulosic Biomass:	13
1.4 Thermo-chemical conversion of biomass	15
1.5 Biomass analysis	22
Chapter 2. Motivation for Thesis	24
2.1 Introduction	24
2.2 GHG emission from Agriculture	25
2.3 Cattle Manure as Source of Energy	25
2.4 Indoor air pollution due to combustion of dried dung.....	26
2.5 Dried Cattle dung as feedstock for thermochemical process and analysis of ash	27
Chapter 3. Chemical Kinetics.....	28
3.1 History and Overview	28
3.2 Rate of Reaction	28
3.3 Factors affecting reaction rate	29
3.4 Solid State Kinetics	31
3.5 Models in solid state kinetics	31
3.6 Data Interpretation and calculation	33
Chapter 4. Thermal Analysis Techniques	35
4.1 Thermo-gravimetric Analysis.....	35
4.2 Differential Scanning Calorimetry	37
Chapter 5. Fuel Analysis	39
5.1 Proximate analysis	39
5.2 Ultimate analysis	41
Chapter 6. Thermal Analysis of Dried Dung	43
6.1 Sample Preparation	43
6.2 Equipment	43
6.3 Pyrolysis	44
6.4 Combustion	49
6.5 Influence of Oxygen Partial Pressure (Partial Oxidation)	51

Chapter 7. Kinetic Modelling of Thermochemical Processes	54
7.1 Introduction	54
7.2 Euler's method	56
7.3 Langmuir Adsorption	57
7.4 Kinetic Model for Pyrolysis	58
7.5 Kinetic Model for Combustion	64
7.6 Kinetic Model for Partial Oxidation	68
Chapter 8 Analysis of Ash	73
8.1 Introduction	73
8.2 Importance of N-P-K in plant growth	73
8.3 Ash composition and usage as fertilizer	73
8.4 P and K analysis	74
8.5 Further Application	75
Conclusion.....	76
References	79

Acknowledgement

I would first like to thank my thesis advisors Professor Francisco Lemos and Amelia Lemos. The door to Prof. Lemos' office was always open whenever I ran into a trouble spot or had a question about my research or writing. He consistently allowed this thesis to be my own work, but steered me in the right the direction whenever he thought I needed it.

I would also like to thank Dr. Klimanek; my supervisor at home university along with Prof. Pikon.

I would like to pay my special thanks KIC Innoenergy for selecting me for this program and giving scholarship for the study. Opportunity to study in multicultural environment really helped me to become a game changer.

My sincere thanks also goes to Mr. Everton Santos, Ms. Bruna Rijo and Mr. Abdullah Saqib for their constant help during experiments.

Finally, I must express my very profound gratitude to my parents and my friends for their unfailing support and continuous encouragement throughout my years of study and through the process of researching and writing this thesis. This accomplishment would not have been possible without them. Thank you.

Abstract

Greenhouse gas (GHG) emissions from anthropogenic sources is a major environmental concern for the whole globe. Among the various sources of GHG emissions are Industries, energy and electricity production, agriculture and building and transportation. Amongst the resources that have the highest likelihood of being controlled easily is Farming. Cattle breeding industry emits 14% of the world's greenhouse emission; among which 10% is due to natural enteric fermentation and 4% is due to mismanagement of cattle dung and urine.

Cattle dung, is a lignocellulosic material with high moisture and high ash content, which has the potential of energy generation or conversion. Currently, for energy conversion it is utilized in anaerobic digestion and direct combustion process. Anaerobic digestion generates biogas but has a low carbon conversion efficiency, and requires removal of hydrogen sulfide and ammonia from the biogas before use. Direct combustion is only used in developing countries as cheap energy resources for cooking and heating purposes in low efficiency stoves which causes many chronic respiratory diseases and deaths due to poor indoor air quality. Cattle dung is a cheap source of fuel which can be utilized in various thermochemical conversions to convert it into various solid, liquid and gaseous fuels, which are more efficient and high in energy density. As, the fuel has to be dried for thermochemical conversion, dried cattle dung is used for experiments.

In this thesis, the kinetics of three major types of thermochemical processes; pyrolysis, combustion and gasification (partial oxidation) is studied. Ultimate and proximate analysis of dried dung is performed to predict behavior of fuel. Thermo gravimetric (TG), Differential Thermo gravimetric (DTG) and Differential Scanning Calorimetry (DSC) techniques are used to understand effect of heat rate and flow rate in thermochemical conversion processes. For combustion experiments, air is used. For pyrolysis experiments, nitrogen is used to provide an inert media. To study the influence of oxygen partial pressure a mixture of air and nitrogen is used. Kinetic data were gathered for all the experiments with variation in heat rates and discussed in following chapters.

Results of thermogravimetric experiments for combustion and pyrolysis at 5 , 20, 50 and 100 °C/min heating rates and for oxidation with different partial pressures of oxygen, ranging $p^{O_2} = 0.21, 0.105, 0.0525, 0.021, 0.0105$ atm, are used for kinetic modelling to estimate the activation energy and other kinetic parameters of the fuel. It is assumed that all the reactions are of first order during modelling.

Cattle dung ash that results from the thermochemical processes contains a high amount of mineral matter, majorly silica. It contains various plant nutrition elements like phosphorus (P), potassium (K), magnesium (Mg), sodium (Na) etc. Phosphorus and potassium being a major element for plant development, an experiment is performed to estimate the elemental P and K content in ash. From the experimental content, usage of ash is discussed.

Keywords: Combustion, Pyrolysis, Partial Oxidation, Thermogravimetry, Dried dung

Resumo

As emissões de gases com efeito estufa (GEE) de origem antropogénica são uma grande preocupação ambiental para todo o globo. Entre as várias fontes de emissões de GEE, estão a produção Industrial, de energia e eletricidade, a agricultura, construção e os transportes. A Agricultura está entre os recursos que podem ser mais facilmente controlados. A Indústria pecuária é responsável, por 14% das emissões de gases com efeito de estufa a nível mundial; entre os quais 10% é devido à fermentação entérica natural e 4% é devido à má gestão de dejetos de gado e na urina.

O estrume produzido pelo gado é um material lignocelulósico com alta humidade e um elevado teor de cinzas, e tem potencial para geração de energia ou conversão. Atualmente, para a produção de energia são utilizados os processos de digestão anaeróbica e de combustão direta. A digestão anaeróbia tem uma baixa eficiência de conversão carbono e obriga à remoção de sulfureto de hidrogénio e da amónia do biogás produzido antes do seu uso. A combustão direta só é usada em países em vias de desenvolvimento, como recurso energético barato para cozinhar e para fins de aquecimento em fogões de baixa eficiência, o que causa muitas doenças respiratórias crónicas e mortes devido à má qualidade do ar interior. O estrume de gado é uma fonte barata de combustível que pode ser utilizada através de várias conversões termoquímicas para convertê-lo em diferentes combustíveis sólidos, líquidos ou gasosos, que são mais eficientes e de maior densidade energética. Como, o combustível tem que ser seco para a conversão termoquímica, estrume de gado seco é utilizado para as experiências neste trabalho.

Nesta tese, foi estudada a cinética de três tipos principais de processos termoquímicos; pirólise, combustão e gaseificação (oxidação parcial). Foi feita análise elementar e global do estrume seco para prever o comportamento do combustível. Foram utilizadas técnicas Termogravimétricas (TG), de Gravimetria Térmica Diferencial (DTG) e de Calorimetria Diferencial de Varredura (DSC) para analisar o efeito da taxa de aquecimento e fluxo de gás nos processos de conversão termoquímica. Para as experiências de combustão foi utilizado ar. Para as experiências de pirólise foi usado azoto para fornecer uma atmosfera inerte. Para estudar a influência da pressão parcial de oxigénio foi utilizada uma mistura de ar e de azoto. Os dados cinéticos foram recolhidos para todos os ensaios variando as taxas de aquecimento e serão discutidos nos capítulos seguintes.

Os resultados das experiências de termogravimetria para a combustão e para pirólise a taxas de aquecimento de 5, 20, 50 e 100 °C / min e para a oxidação parcial com diferentes pressões parciais de oxigénio, que variam de $pO_2 = 0, 21, 0,105, 0,0525, 0,021, 0,0105$ atm, são utilizados para a modelação cinética para estimar a energia de activação e outros parâmetros cinéticos do combustível. Supõe-se que todas as reacções são de primeira ordem.

As cinzas do estrume de gado, produzidas após os processos termoquímicos, contêm uma elevada quantidade de matéria mineral, maioritariamente sílica. Contém também vários elementos essenciais para a nutrição de plantas, como fósforo (P), potássio (K), magnésio (Mg), sódio (Na), etc. Sendo o fósforo e o

potássio elementos importantes para o desenvolvimento das plantas, foi realizada uma experiência para estimar os conteúdos em P e K elementares nas cinzas. A partir dos resultados experimentais, é discutido o uso das cinzas.

Palavras-chave: combustão, pirólise, oxidação parcial, termogravimetria, estrume seco

List of figures

Figure 1 Structure of Cellulose	13
Figure 2 Molecular Structure of a Hemicellulose, Xylan	14
Figure 3 Molecular Structure of Lignin	14
Figure 4 Structure of a Ligno-cellulosic biomass	15
Figure 5 Reaction Paths for wood pyrolysis	17
Figure 6 Types of Fixed bed gasifiers a) updraft b) downdraft and c) cross-draft	20
Figure 7 Global Greenhouse Gas Emission by Economic Sector	24
Figure 8 TG Diagram	35
Figure 9 DTG curve	36
Figure 10 Heat Flux DSC system	37
Figure 11 DSC curve.....	38
Figure 12 TG curves of Pyrolysis of Dung Cake.....	39
Figure 13 TG curve of combustion of charcoal.....	40
Figure 14 Dung cakes used in experiment	43
Figure 15 TA Instruments SDT 2960 Simultaneous DSC-TGA.....	44
Figure 16 Pyrolysis of dung cake at different heat rate.	45
Figure 17 Effect of heat rate on volatiles produced	46
Figure 18 DSC curves of dung cake pyrolysis at different heat rates.....	47
Figure 19 Effect of heat rate on char produced.	47
Figure 20 DSC curves of combustion of char	48
Figure 21 DTG curve for the combustion of the char produced for the pyrolysis experiment at 5 °C/min.	48
Figure 22 DTG curve of combustion of dung cake	50
Figure 23 Comparison of DSC curves of combustion and pyrolysis	50
Figure 24 DTG curves at different heat rates.....	51
Figure 25 DTG curves of partial oxidation of dung cake.....	52
Figure 26 DSC curves of partial oxidation of dung cake.....	53

Figure 27 Comparison of Pyrolysis and oxidation of lignocellulosic biomass	54
Figure 28 DTG curves of partial oxidation of pinewood, xylan, cellulose and lignin at $PO_2 = 0.05$ atm.....	55
Figure 29 Euler's Method	56
Figure 30 Mechanism of the kinetic modelling of pyrolysis.....	60
Figure 31 DTG curves of pseudo components obtained from kinetic modelling of pyrolysis	62
Figure 32 Comparison of TG curves of modelling and experimental values at different heat rates	63
Figure 33 Mechanism of the kinetic modelling of combustion	64
Figure 34 Differential curves of pseudo components obtained from kinetic modelling of combustion	66
Figure 35 Comparison of TG curves of modelling and experimental values at different heat rates	67
Figure 36 Mechanism of the kinetic modelling of partial oxidation	69
Figure 37 Comparison of TG curves of modelling and experimental values at different heat rates	71
Figure 38 Proposed system for future work	78

List of tables

Table 1 Classification of biomass	12
Table 2 Operating parameters and products for pyrolysis process	17
Table 3 Advantages and Disadvantages of various Gasifiers	20
Table 4 Comparison of emissions from combustion of LPG and dried dung	27
Table 5 Proximate Analysis of Dung cake.	40
Table 6 Ultimate Analysis of Dung cake	41
Table 7 Programming for Pyrolysis Experiment.....	44
Table 8 Programming for combustion experiments	49
Table 9 Effect of heat rate on combustion parameters	51
Table 10 Programming for partial oxidation	52
Table 11 Combustion characteristics with change in oxygen flow.....	53
Table 12 Composition of lignocellulosic material in pyrolysis at different heat rates	61
Table 13 Activation energies estimated for the pyrolysis of different pseudo components considered	62
Table 14 Errors and curve fitting associated with pyrolysis modelling	63
Table 15 Composition of lignocellulosic material in combustion at different heat rates	65
Table 16 Activation energies of pseudo components	65
Table 17 Errors and curve fitting associated with combustion modelling	67
Table 18 Values of kinetic parameters of pyrolysis and combustion obtained during modelling	69
Table 19 Composition of lignocellulosic material in partial oxidation at different heat rates	70
Table 20 Errors and curve fitting associated with combustion modelling	70
Table 21 Analysis of cattle manure ash	74
Table 22 Elemental analysis of Phosphorus and Potassium.....	74
Table 23 Comparison of Kinetic parameters of pyrolysis and combustion	77

Chapter 1. Introduction

This chapter contains a brief introduction of chemical composition and energy potential of biomass, as well as an overview of thermochemical processes for biomass conversion. The intention is to place the reader within the framework of this thesis. In the last section motivation of the thesis is mentioned.

1.1 Types of Biomass:

Biomass can be defined as any general hydrocarbon material which can be obtained from biodiversity. Some biomass types also contains significant amount of inorganic species. Sources of biomass can be various natural and derived materials, such as woody and herbaceous species, woody wastes (e.g. from forest thinning and harvesting, timber production and carpentry residues), agricultural and industrial residues, waste paper, municipal solid waste, sawdust, grass, waste from food processing, animal wastes, aquatic plants and industrial and energy crops grown for biomass.[1]

For political and social reasons, other materials such as tires, manufactured from either synthetic or natural rubbers may be included under the category of biomass even though the material is not strictly fully biogenic but considered into municipal solid waste or other waste. [2]

From the biomass to energy conversion point of view, special attention is given to the production of energy crops. Energy crops are produced at relatively high photosynthetic efficiency or high carbohydrate content and other hydrocarbon materials. [3]

Table 1 Classification of biomass [4]

Virgin	Terrestrial biomass	Forest biomass Grasses Energy crops Cultivated crops
	Aquatic biomass	Algae Water plants
Waste	Municipal waste	Municipal solid waste Biosolids, sewage Landfill gas
	Agricultural solid waste	Livestock and manures Agricultural crop residue
	Forestry residues	Bark, leaves, floor residues
	Industrial wastes	Demolition wood, sawdust Waste oil or fa

General classification of biomass depending on the source of origin is shown in table 1. Virgin biomass includes wood, plants, and leaves which are ligno-cellulosic; and crops and vegetables which are generally

carbohydrates. Waste includes solid and liquid wastes (municipal solid waste); sewage, animal, and human waste; gases derived from landfilling; and agricultural wastes. [4]

1.2 Structure of Biomass

The main components of plant biomass are extractives, fiber or cell wall components, and ash. Extractives are substances vegetable or animal tissue that can be separated by treatment with solvents and recovered by evaporation of the solution. They include protein, oil, starch, sugar, and so on. Cell wall provides structural strength to the plant. A typical cell wall is made of cellulose or hemicellulose fibers and lignin. Cellulose or hemicellulose fibers impart strength to the plant structure and lignin holds the fibers together. Ash is the inorganic component of the biomass. [4]

Wood and its residues (ligno-cellulosic biomass) are the dominant form of the biomass resource base. Detailed discussion of structure of ligno-cellulose structure is presented next.

1.3 Structure of Lignocellulosic Biomass:

Lignocellulosic biomass is generally composed of hemicellulose, cellulose, and lignin. These structures are illustrated below:

Cellulose

Cellulose is the primary structural component of cell walls in biomass. The amount of cellulose in lignocellulosic biomass varies from 90% by weight in cotton to about 1/3 for most other plants. Cellulose can be represented by the generic formula $(C_6H_{10}O_5)_n$ and it is a long chain polymer with a high degree of polymerization ($\sim 10,000$) and a large molecular weight ($\sim 500,000$). [4]

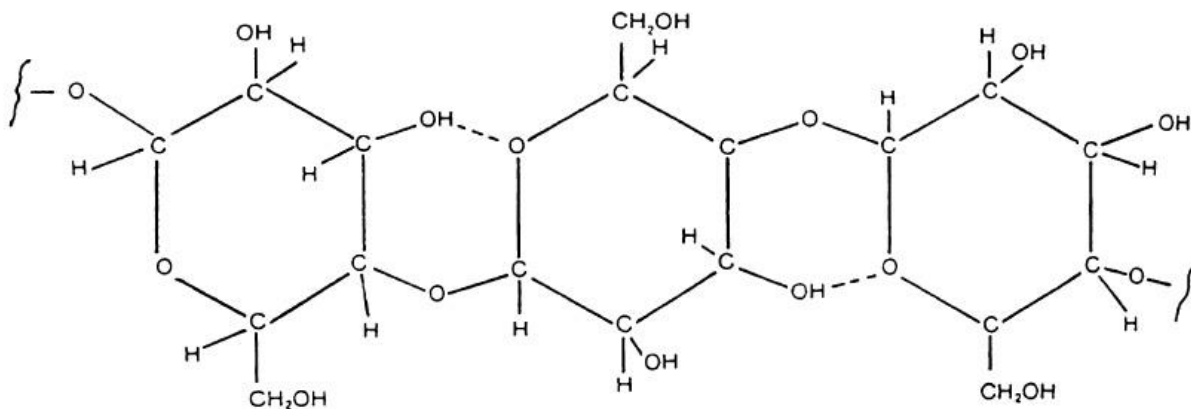


Figure 1 Structure of Cellulose [4]

Cellulose has a crystalline structure of thousands of units, which are made up of many glucose molecules. This structure gives it high strength, permitting it to provide the skeletal structure of most terrestrial biomass. Cellulose is primarily composed of d-glucose, which is made of six carbons or hexose sugars as shown in figure 1.

Hemicellulose

Hemicellulose is another constituent of the cell walls of a plant. While cellulose is of a crystalline, strong structure that is resistant to hydrolysis, hemicellulose is mostly a random, amorphous structure with little strength (figure 2). Hemicellulose is a group of carbohydrates with a branched chain structure and a lower degree of polymerization (~100–200), and may be represented by the generic formula $(C_5H_8O_4)_n$. [4]

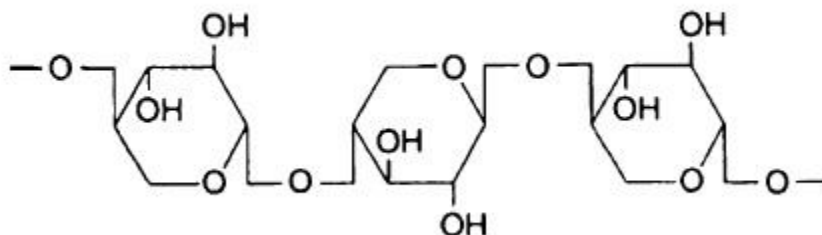


Figure 2 Molecular Structure of a Hemicellulose, Xylan [4]

Molecular structure of a typical hemicellulose called as Xylan is shown in figure 2. Structure and composition of hemicellulose varies with different type of biomasses. Most hemicelluloses, however, contain some simple sugar residues like d-xylose (the most common), d-glucose, d-galactose, l-arabinose, d-glucuronic acid, and d-mannose. These typically contain 50 to 200 units in their branched structures.

Lignin

Lignin is a complex highly branched polymer of phenylpropane and is an integral part of the secondary cell walls of plants. It is primarily a three dimensional polymer of 4-propenyl phenol, 4-propenyl-2-methoxy phenol, and 4-propenyl-2,5-dimethoxy phenol [5] shown figure 3.

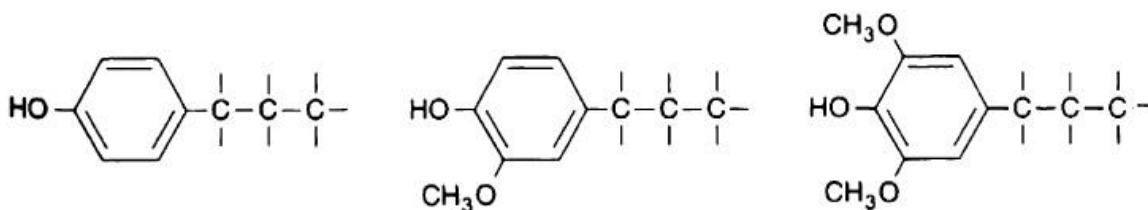


Figure 3 Molecular Structure of Lignin [4]

Lignin is cementing agent for cellulose fibers holding adjacent cells together. The dominant monomeric units in the polymers are benzene rings. It is similar to the glue in a cardboard box, which is made by gluing together papers. Lignin is highly insoluble, even in sulphuric acid. A typical hardwood contains about 18 to 25%, while a softwood contains 25 to 35% by dry weight [4].

Altogether, these three components combine in a ligno-cellulosic biomass is shown in figure 4.

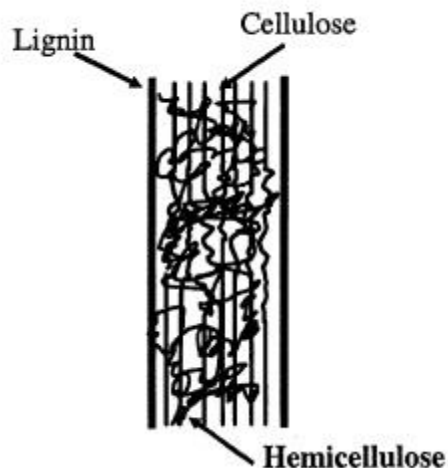


Figure 4 Structure of a Ligno-cellulosic biomass[4]

1.4 Thermo-chemical conversion of biomass

In general, Lignocellulosic biomass has a lower density when compared to coal. Also biomass contains high volatile matter that can be transformed to other gaseous and liquid fuels through thermochemical processes. Thermochemical conversion includes combustion, thermal gasification, and pyrolysis. In this section various thermo-chemical energy conversion processes of biomass is discussed.

Combustion

Combustion is the direct utilization of biomass to produce energy and it can be said that civilization began with the discovery of fire, which is closely linked to the combustion of biomass. In the beginning, forest wood was used for cooking and heating. Combustion is an exothermic reaction between the hydrocarbons in biomass and oxygen. After complete combustion, biomass is mainly converted to H_2O and CO_2 .

Present time, biomass is the major source in developing countries for their energy needs. Biomass still provides heat for cooking and warmth, especially in rural areas. Heat and electricity are two principal forms of energy derived from biomass. District or industrial heating is also produced by steam generated in

biomass fired boilers. Pellet stoves and log-fired fireplaces are as well a direct source of warmth in many cold-climate countries. Electricity, the foundation of all modern economic activities, can also be generated from biomass combustion. [4]

Biomass is used either as a direct fuel or as a supplement to fossil fuels in a boiler. The latter option is becoming increasingly common as the fastest and least-expensive means for decreasing the emission of non-biogenic carbon dioxide from an existing fossil fuel plant [6]. This option is called co-firing.

Pyrolysis

Charcoal, a smokeless fuel used for heating purpose, has been produced by pyrolysis from wood biomass for thousands of years. The demerits of early pyrolysis technology are slow production, low energy efficiency and excessive air pollution. So, development of technology for recovery of the maximum possible energy from a particular type of biomass is continuing to appear as an important step towards a profitable investment. [7]

Pyrolysis is simply the decay of the initial solid fuel into gases and liquids without an oxidizing agent by the influence of heat. The process of pyrolysis of biomass is very complicated and consists of both concurrent and successive reactions when biomass is heated in a non-reactive atmosphere. In this process, thermal decay of organic components in biomass starts at 350 °C–550 °C and goes up to 700 °C–800 °C in the absence of oxygen [8]. The long chains of carbon, hydrogen and oxygen compounds in biomass crack into smaller molecules in the form of gases, condensable vapors (tars and oils) and solid charcoal under pyrolysis conditions. Rate and extent of decomposition of each of these components depends on reactor (pyrolysis) temperature, biomass heating rate, pressure, reactor configuration, feedstock as well as all other process parameters [7].

Figure 5 shows possible reaction pathways for the pyrolysis of wood biomass. Lanzetta and Blasi found that, at the beginning of the pyrolysis (250 °C–300 °C) process, most of the volatiles are released at a rate 10 times faster than the next step. In next step, cracking of higher carbon chains of hydrocarbon takes place which results mostly into condensable bio-liquids' vapors. This bio-oil, char and gas that are produced are reactive substances which generally re-polymerizes after weeks or months [9].

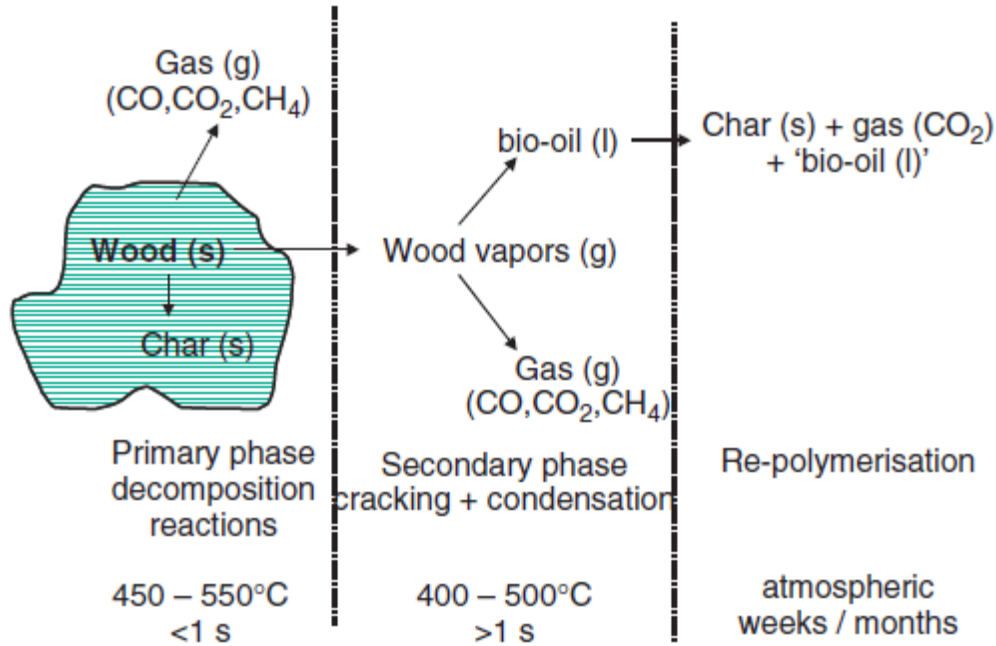


Figure 5 Reaction Paths for wood pyrolysis [10].

Pyrolysis Classification

Depending on the operating condition, pyrolysis can be classified into three main categories: slow, fast and flash pyrolysis. These differ in process temperature, heating rate, solid residence time, biomass particle size, etc. Relative distribution of products is dependent on pyrolysis type and pyrolysis operating parameters as shown in Table 2. In addition, different types of pyrolysis processes are described in the following three sub-sections.

Table 2 Operating parameters and products for pyrolysis process [11, 12].

Pyrolysis Process	Solid Residence Time(s)	Heating Rate (K/s)	Particle Size (mm)	Temperature (K)	Product Yield (%)		
					Oil	Char	Gas
Slow	450-550	0.1-1	5-50	550-950	30	35	35
Fast	0.5-10	10-200	<1	850-1250	50	20	30
Flash	<0.5	>1000	<0.2	1050-1300	75	12	13

Slow Pyrolysis

Slow pyrolysis has been used since thousands of years for char production at low temperatures and low heating rates. In this process, the vapour residence time is high (5 min to 30 min) and components in the vapour phase continue to react with each other which results in the preferential formation of solid char and other liquids [13].

However, slow pyrolysis has some technological constraints which makes it unlikely to be suitable for good quality bio-oil production. Cracking of the primary product in the slow pyrolysis process occurs because of high residence time and could adversely affect bio-oil yield and quality. Also, longer residence time and lower temperature may demand extra energy input [14].

Fast Pyrolysis

In the fast pyrolysis process, biomass is rapidly heated to a high temperature in the absence of oxygen. On a weight basis, fast pyrolysis produces 50%–65% of oily products (oil and other liquids) with 15%–25% of solids (mainly biochar and ash) and 10%–30% of gaseous phase depending on the biomass used. The production of liquids is usually gained from biomass in high (850-1250 K) temperature, high heating rate and short resident time environment. General characteristics of the fast pyrolysis process are high heat transfer and heating rate, very short vapour residence time, rapid cooling of vapors and aerosol for high bio-oil yield and precision control of reaction temperature [15].

Fast-pyrolysis technology is popular in producing liquid fuels and a range of commodity chemicals. This liquid product can be easily and economically transported and stored, thereby individualizing handling of solid biomass from utilization [16]. Fast Pyrolysis has potential to supply various valuable chemicals that offer the attention of much higher added value than fuels. Fast pyrolysis technology can have relatively low investment costs and high energy yields compared to other processes, significantly on a small scale. Production of bio-oil through fast pyrolysis has received more attraction in recent year due to the following potential advantages [17, 18]:

- Renewable fuel for power generation turbine, boiler, engine and industrial processes;
- CO₂ neutral and low cost;
- Utilization of waste materials like forest residue, municipal and industrial waste, etc.;
- Economically viable storability and transportability of liquid fuels compared to biomass;
- High energy density compared to atmospheric biomass gasification fuel gases;
- Possibility for separating minerals from ashes from liquid fuel production site to be recycled to the soil as a nutrient;
- Secondary conversion to transportation fuels, additives or special chemicals;
- Primary separation of the sugar and lignin fractions in biomass with subsequent further upgrading.

Flash Pyrolysis

The flash pyrolysis of biomass is a process for the production of fuels (solid, liquid and gaseous) from biomass which can achieve up to 75% of bio-oil efficiency. This process can be characterized by rapid devolatilization in inert atmosphere, high heating rate of small biomass particles, high reaction temperatures between 450 °C and 1000 °C and very short gas residence time (less than 1 s) [19]. However this process has some technological limitations, like poor thermal stability and corrosiveness of the oil and presence of solids in the oil, Increase of the viscosity over time by catalytic action of char, alkali concentrated in the char dissolves in the oil and production of pyrolytic water [20].

Gasification

The production of generator gas (alias producer gas and syngas) through gasification process is partial oxidation of biomass and takes place at temperatures of about 1000 °C. The reactor is called a Gasifier [4].

The combustion products from complete combustion of biomass generally contain nitrogen, water vapor, carbon dioxide and surplus of oxygen. However in gasification where conditions are sub-stoichiometric, there is a surplus of solid fuel (incomplete combustion) the products of combustion are combustible gases like Carbon monoxide (CO), Hydrogen (H₂) and traces of Methane and non-useful products like tar and dust. The production of these gases occurs by reaction of water vapor and carbon dioxide through a glowing layer of charcoal. Thus the key to Gasifier design is to create conditions such that biomass is reduced to charcoal and charcoal is converted at suitable temperature to produce CO and H₂. [20]

Types of Gasifiers

Generally for biomass small scale fixed gasifiers are used. Since there is an interaction of air or oxygen and biomass in the gasifier, they are classified according to the way air or oxygen is introduced in it. There are three types of fixed bed gasifiers as shown in Figure 6; Downdraft, Updraft and Cross-draft. And as the classification implies updraft gasifier has air passing through the biomass from the bottom to the top and the combustible gases come out from the top of the gasifier.

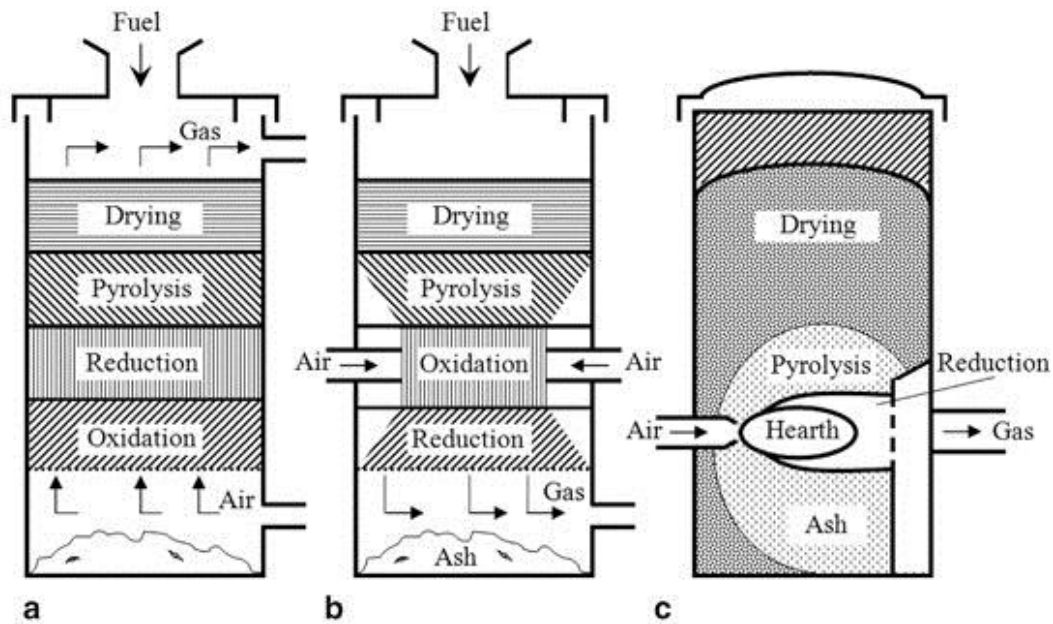


Figure 6 Types of Fixed bed gasifiers a) updraft b) downdraft and c) cross-draft [22].

Similarly in the downdraft gasifier the air is passed in the gasifier in the downdraft direction. With slight variation almost all the gasifiers fall in the mentioned category. The choice of one type of gasifier over other is decided by the fuel, its final available form, its size, moisture content and ash content. Table 3 lists therefore, the advantages and disadvantages generally found for various classes of gasifiers [21].

Table 3 Advantages and Disadvantages of various Gasifiers [21].

Sr. No.	Gasifier Type	Advantages	Disadvantages
1	Updraft	<ul style="list-style-type: none"> Small pressure drop Better thermal efficiency Lower tendency towards slag formation 	<ul style="list-style-type: none"> Great sensitivity to tar and moisture and moisture content of fuel Poor reaction capability with heavy gas load
2	Downdraft	<ul style="list-style-type: none"> Flexible adaptation of gas production to load Lower sensitivity to dust and tar content of fuel 	<ul style="list-style-type: none"> Design tends to be taller. Not viable for very small particle size of fuel
3	Cross-draft	<ul style="list-style-type: none"> Short design height Very fast response time to load Flexible gas production 	<ul style="list-style-type: none"> Very high sensitivity to slag formation High pressure drop

Process Zones

Regardless of the type of gasifier, four distinct areas can be identified inside the equipment, associated with the different processes that take place in a gasifier as the fuel makes its way to gasification [21]. They are:

- a) Drying of fuel – moisture evaporation
- b) Pyrolysis – tar and other volatiles are driven off
- c) Combustion – oxidation of char and volatiles
- d) Reduction – reduction of char and volatiles into syngas

Though there is a considerable overlap of the processes, each can be assumed to occupy a separate zone where fundamentally different chemical and thermal reactions take place as shown in figure 6.

Reaction Chemistry

The following major reactions take place in drying, combustion, pyrolysis and reduction zone,

Drying zone:

In the drying zone the main process is of drying of wood. Wood entering the gasifier has a moisture content of 10-30%. Various experiments on different gasifiers in different conditions have shown that on average the condensate formed is 6-10% of the weight of gasified wood. Some organic acids also come out during the drying process. These acids give rise to corrosion of the gasifiers.

Combustion zone:

The combustible substance of a solid fuel is usually composed of carbon, hydrogen and oxygen. In complete combustion, carbon dioxide is obtained from carbon in fuel and water is obtained from the hydrogen, generally as steam. The combustion reaction is exothermic. The main reactions, therefore, are:



Pyrolysis zone:

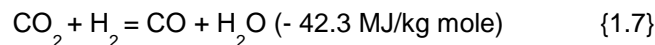
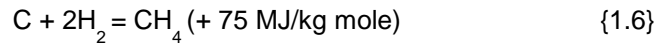
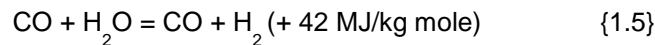
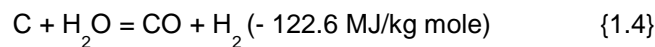
Biomass pyrolysis is a complicated process that is still not completely understood. The products depend upon temperature, pressure, residence time and heat losses. However following general remarks can be made about them.

Up to the temperature of 200 °C only water is driven off. Between 200 and 280 °C, carbon dioxide, acetic acid and water are given off. The real pyrolysis, which takes place between 280 to 500 °C, produces large quantities of tar and gases containing carbon dioxide. Besides light tars, some methanol is also formed. Between 500 to 700 °C the gas production is small and contains hydrogen. [21]

Thus it is easy to see that updraft gasifier will produce much more tar than downdraft one. In downdraft gasifier the tars have to go through combustion and reduction zone and are partially broken down. Since most of fuels like biomass and waste do have large quantities of tar, downdraft gasifier is preferred over others.

Reduction zone:

The products of partial combustion (water, carbon dioxide and partially cracked pyrolysis products) now pass through a red-hot charcoal bed where the following reduction reactions take place.



Reactions (1.3) and (1.4) are main reduction reactions and being endothermic have the capability of reducing gas temperature. Consequently the temperatures in the reduction zone are normally 800-1000 °C. The lower the reduction zone temperature, the lower is the calorific value of gas.

1.5 Biomass analysis

Thermal design of a biomass energy system necessarily needs the composition of the fuel as well as its energy content. The following three primary properties describe its composition and energy content: (1) ultimate analysis, (2) proximate analysis, and (3) heating values.

Ultimate Analysis

Here, the composition of the biomass fuel is expressed in terms of its basic elements except for its moisture (M) and inorganic constituents (ASH). A typical ultimate analysis is

$$C + H + O + N + S + ASH + M = 100\% \quad (1.1)$$

Here, C, H, O, N, and S are the weight percentages of carbon, hydrogen, oxygen, nitrogen, and sulfur, respectively, in the fuel. Not all fuels contain all of these elements. The moisture or water in the fuel is expressed separately as M. Ultimate analysis is often just elemental analysis. Here, hydrogen or oxygen in the ultimate analysis includes hydrogen and oxygen present in the organic components of the fuel.

Proximate Analysis

Proximate analysis gives the composition of the biomass in terms of gross components such as moisture (M), volatile matter (VM), ash (ASH), and fixed carbon (FC). The moisture and ash determined in proximate analysis refer to the same moisture and ash determined in ultimate analysis. The volatile matter of a fuel is condensable and non-condensable vapor released when the fuel is heated. Fixed carbon is solid carbon in the biomass that remains in the char in the pyrolysis process after devolatilization. Summation of all the content present by weight percentages in proximate analysis must be 100%.

Higher Heating Value

Higher calorific value (HCV) is defined as the amount of heat released by the unit mass or volume of fuel (initially at 25 °C) once it is combusted and the products have returned to a temperature of 25 °C. It includes the latent heat of vaporization of water.

To find HCV from ultimate analysis of fuel, CY Yin has suggested equation (1.2) of Channiwala and Parikh [23]. Equation is on dry basis which doesn't account for inherited moisture. With help of linear regression analysis, equation (1.2) has comparatively low mean absolute error [24].

$$HCV \left(\frac{MJ}{kg} \right) = 0.3491C + 1.1783H + 0.1005S - 0.1034O - 0.0151N - 0.0211 * Ash \quad (1.2)$$

Lower Heating Value

The lower calorific value (LCV) is defined as the amount of heat released by fully combusting a specified quantity without considering the heat of vaporization of the water in the combustion product. To calculate LCV from HCV following equation (1.3) is used. Enthalpy of evaporation of water at 25 °C is 2.442 MJ/kg.

$$LCV \left(\frac{MJ}{kg} \right) = HCV - (9 * H * \text{Enthalpy of evaporation}) \quad (1.3)$$

Chapter 2. Motivation for Thesis

2.1 Introduction

Division of anthropogenic global greenhouse gas (GHG) emissions by economic sector is shown in below figure 7.

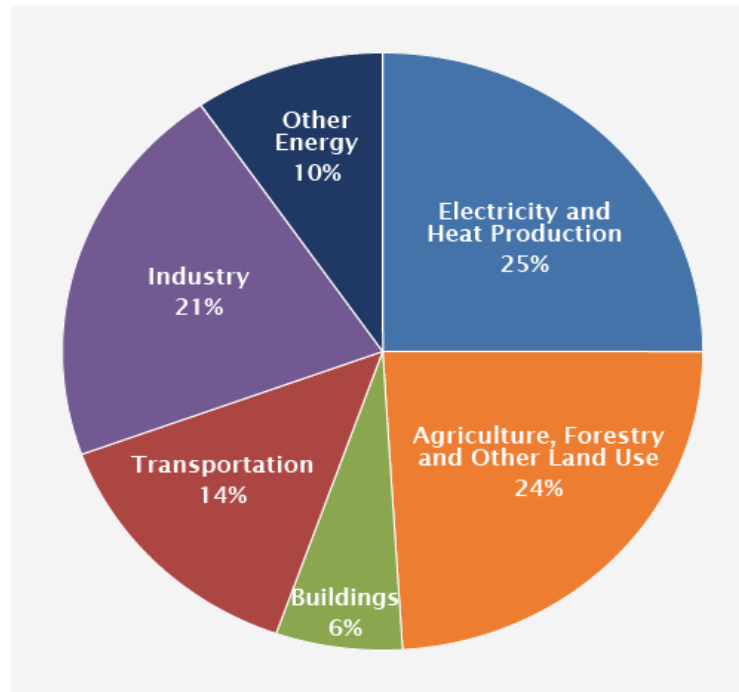


Figure 7 Global Greenhouse Gas Emission by Economic Sector [25].

Electricity and heat production sector is the largest source of GHG emissions and contributes 25% of total GHG emissions. This sector includes burning of coal, natural gas and oil for heat and electricity production. Agriculture, forestry and other land use is the second largest source and contributes 24% of the GHG emissions. GHG emissions from this sector come mostly from cultivation of crops and livestock and deforestation. Emissions from industry (21% of total) primarily involve combustion of fossil fuels at on-site facilities for energy. This sector also includes emissions from non-combustion activities such as chemical, metallurgical, and mineral transformation processes and emissions from waste management activities.

GHG emissions from transportation (14%) sector includes combustion of fossil fuels for road, rail, air, and marine transportation. GHG emissions from buildings (6%) from on-site energy usage and combustion of fuels for heat in buildings or cooking in homes. Other energy (10%) refers to emissions from the energy sector which are not directly associated with electricity or heat production, such as fuel extraction, refining, processing, and transportation.

From the above mentioned anthropogenic sources of GHG emissions, focus is given to agriculture sector because in this sector, sources of GHG emissions like crop residues, livestock manure etc. can be used as biofuels and their further fermentation or wastage in open atmosphere can be eliminated.

2.2 GHG emission from Agriculture

Now, considering emission profile of different sources in agriculture sector from which GHG is emitted to atmosphere. In the domain of agriculture forest and other land use, agriculture comprises 50% of total emission [26], this means 12% of global emissions. Furthermore, division of agriculture sector emissions from different sub-sectors is shown below in figure 8.

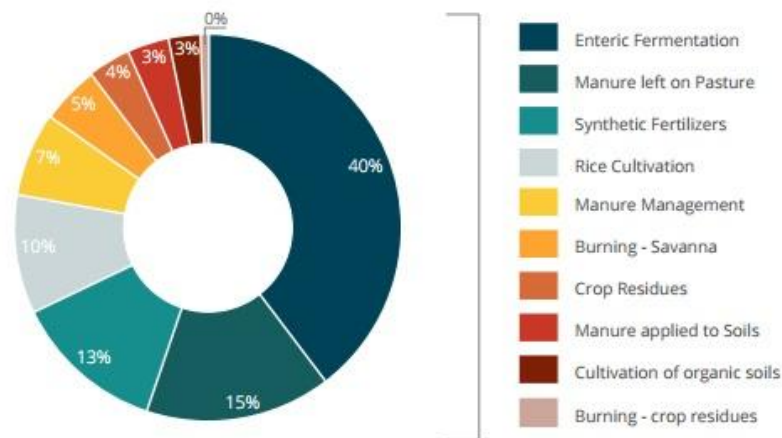


Figure 8 Sub-Sectors of GHG emissions from Agriculture

Emissions from enteric fermentation (40%) consist mostly of methane gas (CH_4) produced in digestive systems of ruminants, which is a natural process and can't be eliminated or controlled. Emissions from manure can be divided into application to cropland as organic fertilizer (3%), left on pasture by grazing animals (15%), or processed in manure management systems (7%). Emissions from farming can be subcategorized into use of synthetic fertilizers (15%), rice cultivation (10%), combustion or fermentation of crop residues (4%), burning-savanna (5%) and cultivation of organic solids (3%) [26].

2.3 Cattle Manure as Source of Energy

Emission from cattle manure corresponds, in total, to 25% of total emission from agriculture, which corresponds to 12% of the global GHG emission. So, directly animal manure consists of 3% of global GHG emissions. This GHG emission can be reduced by proper management and usage of manure.

As received cattle manure is composed of undigested lignocellulose material, moisture (20-60%) and ash (15-20% dry basis). Lignocellulose present in manure is undigested feed to cattle. Manure also contains methanogen bacteria that continuously decomposes lignocellulose into methane and carbon dioxide. If manure is not handled properly, greenhouse gases like methane and carbon dioxide are emitted into atmosphere.

Presently, cattle manure is utilized for energy purposes in two main ways:

1. Anaerobic Digestion
2. Direct Combustion

Anaerobic Digestion

Anaerobic digestion is the most common method for energy conversion from cattle manure. Manure contains the required moisture content for degradation and methanogen bacteria activity that ferments cellulose and hemicellulose into methane (50-70%) and carbon dioxide (20-40%) which is termed as biogas. Structure of lignin is hard to be decomposed by methanogens and remains as it is after digestion. By this method, 50-60% of the organic matter present into manure can be converted into biogas. [27]

It is being widely used because, from the economic point of view, the handling of process and equipment used is relatively simple and further utilization of waste as organic fertilizer. But there are demerits to this process, like low carbon conversion efficiency, necessity of removal of hydrogen sulfide and ammonia from biogas before use [28].

Direct Combustion

As received cattle manure contains a high amount of moisture which needs to be removed by drying it before use any thermochemical conversion processes. Dried dung is sometimes called “dung cake”. Combustion of dried cattle dung is widely practiced in developing countries in Asia, Africa and South America for cooking and heating, as it is an inexpensive source of fuel. In these places, cattle dung is dried with heat from the sun. Incomplete combustion of dried dung releases harmful volatile organic compound, which causes indoor air pollution and results into respiratory diseases. In India, every year 200,000 people die because of indoor air pollution where dried dung is extensively used as fuel for cooking and heating [29].

2.4 Indoor air pollution due to combustion of dried dung

Indoor air pollution is the degradation of indoor air quality by harmful chemicals and other materials. In developing countries, comparatively, the level of indoor air pollution is higher due to usage of lower grade

biomass as fuel for cooking and heating. Indoor air pollution from solid fuels accounted for 3.5 million deaths and 4.5% global daily-adjusted life year in 2010; it also accounted for 16% particulate matter pollution. [30]

Dried dung is a popular fuel for cooking and heating purposes in developing countries. Direct combustion of this fuel degrades indoor air quality. Amongst all general woody biomass, dried dung causes the maximum amount of indoor air pollution. [32]

Comparison of average emissions of various pollutant gases during 24 hours of exposure from combustion of Liquefied Petroleum Gas (LPG) and dried dung is shown in table 4. LPG is considered a very good fuel for cooking as it has very low harmful emissions. From table 4, it can be seen that dried dung has more than 10 times higher emissions than LPG.

Table 4 Comparison of emissions from combustion of LPG and dried dung [30, 31, 32]

Pollutant	LPG	Dried dung
Carbon monoxide (mg/m ³)	14	144
Polyaromatic hydrocarbons (mg/m ³)	0.13	3.56
Formaldehyde (mg/m ³)	68	670
Suspended particulate matter (mg/m ³)	-	2.8

This indoor air pollution can be prevented by changing the way of usage of the fuel. Dried dung can be converted to various other types of solid, liquid and gaseous fuels by thermochemical conversion processes like pyrolysis, gasification, torrefaction etc.

2.5 Dried Cattle dung as feedstock for thermochemical process and analysis of ash

Dried cattle dung's thermochemical conversion has not been studied much due to the popularity of the anaerobic digestion process. Also, to cope with indoor air pollution from combustion of dried dung, study of thermochemical processes is necessary. So, in this thesis, analysis of various kinetic parameters to describe pyrolysis, combustion and gasification is studied. Also, dried cattle dung ash, which is a by-product of gasification and combustion, contains a significant amount of phosphorus and potassium which is essential plant feed and, thus, can be further used as fertilizers. So, analysis of the ash is also done to find out phosphorus and potassium content, which are of interest as fertilizer ingredients.

Chapter 3. Chemical Kinetics

Chemical kinetics is the study of rates of chemical reactions. Chemical kinetics is also known as reaction kinetics. Chemical kinetics includes the study of how various experimental conditions can influence the rate of a chemical reaction and gain information about the reaction mechanism and transition rates, as well as the construction of mathematical models that can describe the characteristics of a chemical reaction. [33]

3.1 History and Overview

Cato Guldberg and Peter Waage presented general theory of dependency of reaction rates on concentrations. It was the first fundamental equation of chemical kinetics. Later on, Van Hoff studied chemical dynamics and published his famous "Etudes de dynamique chimique". He was awarded the first Nobel Prize in Chemistry "in recognition of the extraordinary services he has rendered by the discovery of the laws of chemical dynamics and osmotic pressure in solutions" in 1901. [33]

From the studies of Van Hoff, it was understood that chemical kinetics deals with the experimental determination of reaction rates from which rate laws and rate constants are derived. Relatively simple rate laws exist for zero order reactions for which reaction rates are independent of concentration, first order reactions, and second order reactions, and can be derived for others.

Elementary reactions obey the law of mass action, but the rate law of stepwise reactions has to be derived by integrating the rate laws of the various elementary steps which becomes more complex. In consecutive reactions, the rate-determining step often determines the kinetics. The activation energy for a reaction can be experimentally estimated by resorting to the Arrhenius equation or to the Eyring equation. The main factors that influence the reaction rate include: the physical state of the reactants, the concentrations of the reactants and products, the temperature at which the reaction occurs, and whether or not any catalysts are present in the reaction.[33]

3.2 Rate of Reaction

Before starting with reaction rates, it is necessary to understand reaction mechanism. For a reaction to occur, there are three conditions shown below, has to be satisfied

1. Molecules or atoms of reactants must collide with each other.
2. The molecules must have sufficient energy (Activation energy) to initiate the reaction.
3. In some cases orientation of molecules during the collision must also be considered. [34]

Imagine a general chemical reaction,

$$\sum v_i * A_i = 0 \quad (3.1)$$

Where v_i is stoichiometric coefficient of product or reactant and A_i is product or reactant. By convention, stoichiometric coefficient for products are positive and for reactants are negative and $i = 1, 2, 3, \dots, n$ where n is the number of species involved. With this definition of the stoichiometric coefficients, if we symbolize the rate of a reaction by R , then the relation of R with the change of concentrations of the species in a batch reactor:

$$R = \frac{1}{v_i} * \frac{d[A_i]}{dt} \quad (3.2)$$

The rate is negative when i represent a reactant and positive when i represent a product.

Rate of reaction can also be expressed, empirically, as,

$$R = k * \sum [A_i]^{\alpha_i} * [X_i]^{\beta_i} \quad (3.3)$$

Here, the A_i are the reactants, the X_i are substances that are not reactants but do influence the rate, α_i and β_i are coefficients that are not necessarily related to the stoichiometric coefficients v , and k is a rate constant.

3.3 Factors affecting reaction rate

Nature of the reactants

Depending upon substances that are reacting, the reaction rate varies. Acid/base reactions, the formation of salts, and ion exchange are fast reactions. When covalent bond formation takes place between the molecules and when large molecules are formed, the reactions tend to be slower. Nature and strength of bonds in reactant molecules greatly influence the rate of its transformation into products [33].

Physical state

The physical state (solid, liquid, or gas) of a reactant is also an important factor of the rate of change. When reactants are in the same phase, as in aqueous solution, thermal motion brings them into contact. However,

when they are in different phases, the reaction is limited to the interface between the reactants. Reaction can occur only at their area of contact; in the case of a liquid and a gas, at the surface of the fluid. Vigorous shaking and stirring may be needed to bring the reaction to completion. This means that the more finely divided a solid or liquid reacting is, the greater its surface area per unit volume and the more contact it will have with the other reactant, thus the faster the reaction. Further, homogenous reactions usually take place faster than heterogeneous reactions [33].

Concentration

The reactions are due to collisions of reactant species. The frequency with which the molecules or ions collide depends upon their concentrations. The more crowded the molecules are, the more likely they are to collide and react with one another. Thus, an increase in the concentrations of the reactants will usually result in the corresponding increase in the reaction rate, while a decrease in the concentrations will usually have a reverse effect. For example, combustion will occur more rapidly in pure oxygen than in air (21% oxygen) [33].

Temperature and Arrhenius equation

Temperature usually has a major effect on the rate of a chemical reaction. Molecules at a higher temperature have more thermal energy. Although collision frequency is greater at higher temperatures, this alone contributes only a very small proportion to the increase in rate of reaction. Much more important is the fact that the proportion of reactant molecules with sufficient energy to react (energy greater than activation energy: $E > E_a$) is significantly higher and is explained in detail by the Maxwell–Boltzmann distribution of molecular energies [34].

The **Arrhenius equation** relates the specific rate constant to the absolute temperature.

$$k = A e^{\frac{-E_a}{RT}} \quad (3.4)$$

where E_a is called the *activation energy* and A is the *pre-exponential factor*. As seen from the rate can have a very strongly increasing (exponential) function of temperature, depending on the magnitude of the activation energy E . This equation works well for elementary reactions, and it also works reasonably well for global reactions over a relatively narrow range of temperatures in the absence of mass-transfer limitations. The Arrhenius form represents an energy barrier on the reaction pathway between reactants and products that has to be overcome by the reactant molecules. [34]

3.4 Solid State Kinetics

Here, in this thesis, kinetic parameters of thermochemical conversion processes such as gasification, pyrolysis and combustion are to be found. Feedstock for this processes is dried cattle dung which is a solid fuel and it reacts with gaseous substances like air and nitrogen. For these kind of reactions knowledge of solid state kinetics is required.

A rate law for an elementary solid state reaction could depend on factors such as rate of nuclei formation, interface advance/retreat, diffusion, and/or geometrical shape of solid particles. These factors lead to several decomposition models that do not have an exact parallel in homogenous kinetics. Kinetic equations for reactant conversion fraction of X is expressed as: [35]

$$\frac{dX}{dt} = k f(X) \quad (3.5)$$

By adding value of k from equation (3.4), we get

$$\frac{dX}{dt} = A e^{\frac{-E_a}{RT}} f(X) \quad (3.6)$$

Equation (3.6) will be further used in kinetic modelling in later stage of the report.

A model is a theoretical, mathematical description of what occurs experimentally. In solid-state reactions, a model can describe a particular reaction type and translate that mathematically into a rate equation. Many models have been proposed in solid-state kinetics and these models have been developed based on certain mechanistic assumptions. Other models are more empirically based and their mathematics facilitates data analysis with less mechanistic meaning. Therefore, different rate expressions are produced from these models.

3.5 Models in solid state kinetics

Three order based models are commonly implemented to interpret the experimental result which are as follows: [36]

1. VM (Volume Model)
2. GM (Grain Model)
3. RPM (Random Pore Model)

These models have a theoretical basis and involve fewer parameters and give different formulations of the term $f(X)$.

Volume Model (VM)

The VM assumes that a homogeneous reaction occurs throughout the solid bed and that it results in a linear decrease in the reaction surface area with conversion. The overall reaction rate is given by:

$$\frac{dX}{dt} = k_{VM} (1 - X) \quad (3.7)$$

Grain Model (GM)

The GM considers that the agents react on the surface of the non-porous grains or in pore surfaces within the solid [36]. According to different assumptions, the reaction rates in the regime of chemical control can be expressed as:

$$\frac{dX}{dt} = k_{GM} (1 - X)^{2/3} \quad (3.8)$$

Random Pore Model (RPM)

The RPM considers the overlapping of pore surfaces, which results in the reduction of surface area available for the reaction [36]. The general rate equation for this model is:

$$\frac{dX}{dt} = k_{RPM} (1 - X) \sqrt{1 - \psi \ln (1 - X)} \quad (3.9)$$

This model can predict a maximum for the reactivity during the reaction, as it considers the competing effects of pore growth during the initial stages of gasification, and the destruction of the pores due to the coalescence of neighboring pores during the reaction. The RPM contains two parameters, ψ , which is related to the initial pore structure of the solid sample ($X = 0$) and the reaction rate constant, k .

$$\psi = \frac{4 \pi L_0 (1 - \epsilon_0)}{S_0^2} \quad (3.10)$$

Where S_0 , L_0 , and ϵ_0 represent the pore surface area, pore length, and solid porosity, respectively.

3.6 Data Interpretation and calculation

Solid-state kinetics are studied either isothermally or non-isothermally. Many mathematical methods have been developed to interpret experimental data for both heating protocols. These methods generally fall into one of two categories: [35]

- Model-fitting
- Model-free.

Model Fitting Methods:

For these methods, different models are fit to the data and the model giving the best statistical fit is chosen as the model of choice from which the activation energy (E_a) and frequency factor (A) are calculated. Model fitting approach is often used for pyrolysis reaction description. As a result a single set of kinetic parameters is derived for entire range of temperatures and respective extent of reaction. These are called apparent kinetic parameters.

Isothermal model-fitting method:

This method is identical to that in homogeneous phase kinetics. It involves two fits: The first, determines the rate constant (k) of the model that best fits the data while the second determines specific kinetic parameters such as the activation energy (E_a) and frequency factor (A) using the Arrhenius equation.

Non-isothermal model-fitting method:

There are many model fitting methods that extract the three kinetic parameters known as the kinetic triplet (A , E_a and model) from non-isothermal data. These methods were used extensively earlier in solid-state kinetic analysis and they continue to appear. These methods have been critically evaluated and it's been shown that the sole use of these methods is not recommended because:

- They assume a constant kinetic triplet (A , E_a and model).

- They involve fitting three parameters (A , E_a and model) which are determined from a single run (i.e., one heating rate).
- They involve a single heating rate which is not always sufficient to determine reaction kinetics

Model-free methods

Model-free methods calculate the reaction activation energy (E_a) without modelistic assumptions, which is usually done by grouping terms such as the frequency factor (A) and model into the intercept of a linear equation and using the slope of that equation to calculate the activation energy (E_a). The frequency factor (A) can be calculated from the intercept of the linear equation but requires modeling assumptions for such a determination. Therefore, model-free methods usually report only activation energies.

Chapter 4. Thermal Analysis Techniques

In this chapter thermal analysis techniques used for thesis is discussed. Mainly two techniques are used for thermal analysis which are as below:

- Thermo-gravimetric analysis (TGA)
- Differential Scanning Calorimetry (DSC)

4.1 Thermo-gravimetric Analysis

Thermo-gravimetry analysis (TGA) is a technique in which sample weight is measured as a function of temperature. The sample is loaded on a high precision thermo-balance within the furnace and weighed continuously during the course of the heating program. The mass loss associated with a thermal reaction is measured between the inflection points of the TG curve [37]. Typical TG diagram of a solid substance is shown in figure 8. If differential of mass with respect to time is considered and plotted against temperature then the curve is called differential thermo gravimetric curve (DTG). It is often simpler to interpret and resolve thermal events by plotting the DTG than the TG curve.

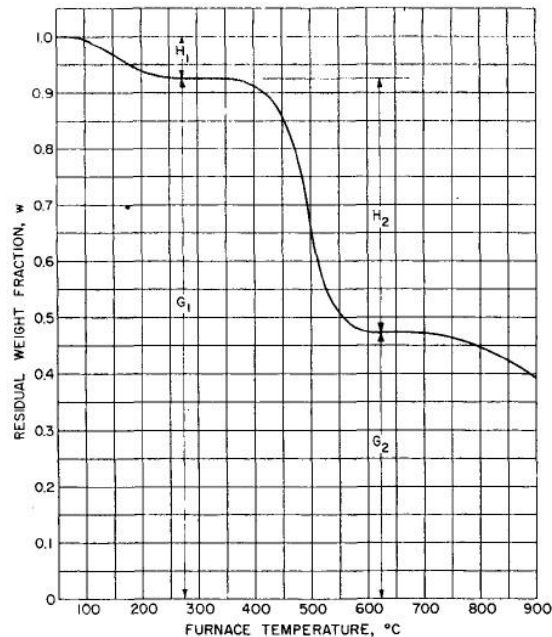


Figure 8 TG Diagram [40].

Certain features in the TGA curve that are not readily seen can be more clearly discerned in the first derivative TGA curve. For example, any change in the rate of weight loss can immediately be seen in the first derivative TGA curve as a trough, or as a shoulder or tail to the peak, indicating two consecutive or overlapping reactions [41].

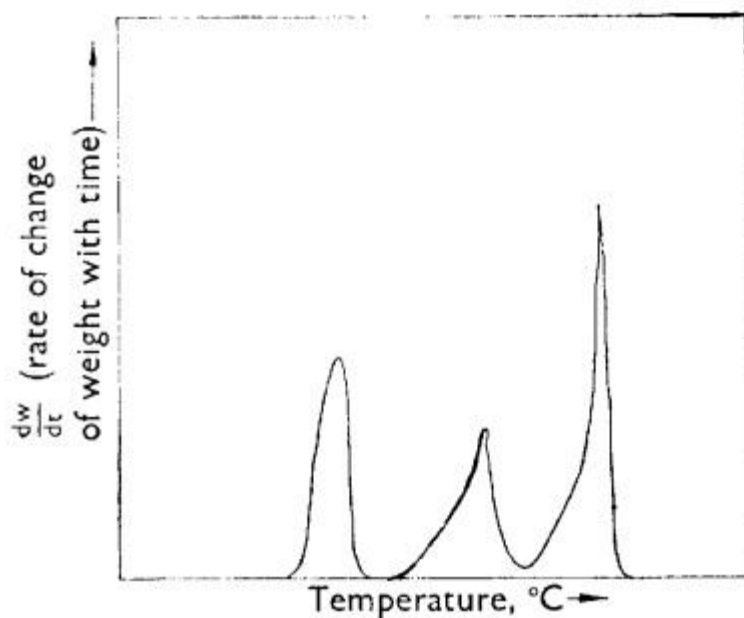


Figure 9 DTG curve [41].

Derivative TG (DTG, units of % mass loss/sec) is thus the preferred method to resolve the position of inflection points against a background of continuous mass loss. The temperature at which mass loss reactions occur in TG instruments is calibrated by measurement of the melting transition temperature of standard reference materials, typically pure metals or salts. [38]

Deviations from the reference temperatures can be corrected in subsequent measurements. Weight calibration is readily achieved using standard weights, and the balance may be calibrated for buoyancy and other effects if necessary. Buoyancy is an apparent mass gain during the initial stage of thermo-gravimetric analysis caused by the aerodynamic drag of gas flow through the furnace [39]. Main uses of TG include measurement of a material's thermal stability and composition. It shows change in mass with respect to temperature.

4.2 Differential Scanning Calorimetry

Differential scanning Calorimetry (DSC) is a technique for measuring the energy added to / removed from a sample and reference as a function of temperature. Two classes of DSC instruments can be distinguished by their principles of operation: power compensation DSC and heat flux DSC. In a heat flux DSC, both sample and reference are heated or cooled by the same single heat source. As the temperature of the furnace is changed according to the applied temperature program, heat is transferred to the sample and reference through the thermoelectric disk. Heat flux DSC shown in figure 10 measures a temperature difference between sample and reference, and the corresponding voltage signal is converted to a heat flow rate (in J s^{-1}). [38]

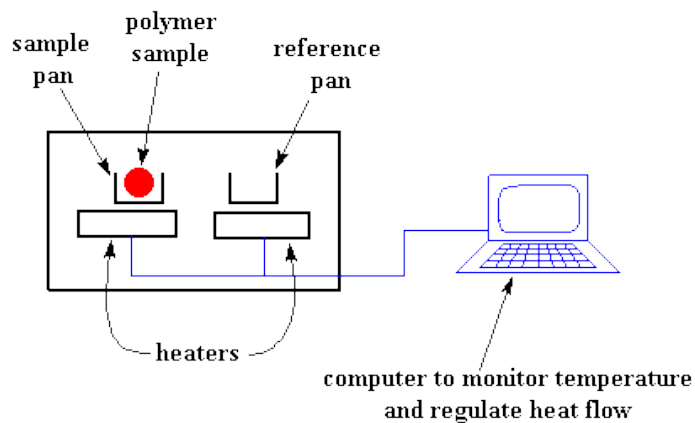


Figure 10 Heat Flux DSC system

[Adapted from <http://pslc.ws/macrog/dsc.htm>]

In power compensation DSC, the objective is to establish a near-zero temperature difference between the sample and reference materials as the two specimens are subjected to identical temperature regimes. The sample and reference are situated in two separate, identical furnaces and the same temperature is maintained for both. The differential power input required to compensate for temperature deviations between the two cells is recorded, and the energy required to do this is a measure of the enthalpy or heat capacity changes in the sample relative to the reference. DSC measures not only endothermic and exothermic effects, but also changes in sample heat capacity as a function of temperature, but for reliable measurements of heat fluxes, each calorimeter must be calibrated for its thermal resistance, heat capacity, and temperature [38].

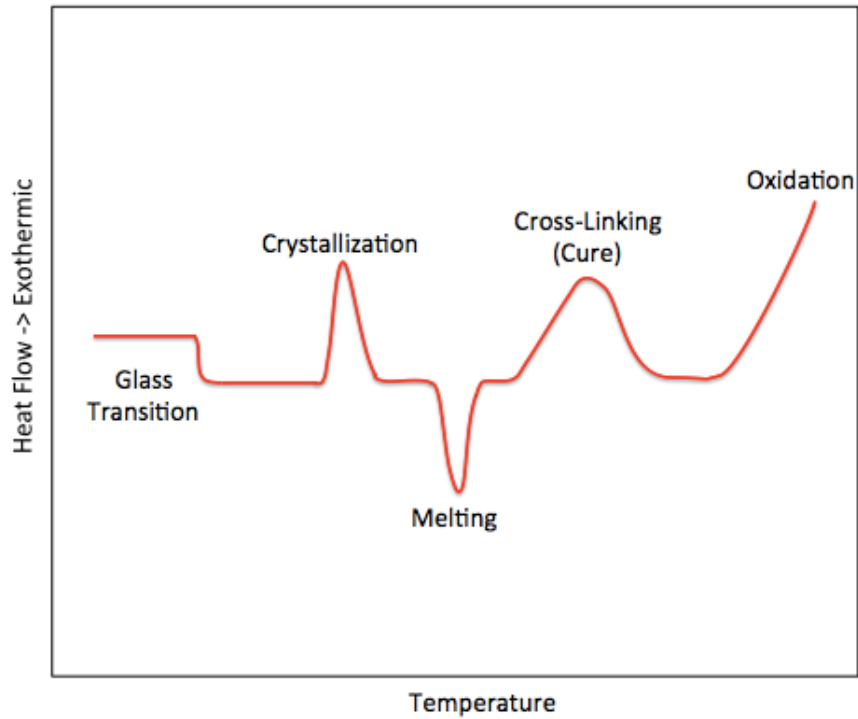


Figure 11 DSC curve

[Adapted from <http://archive.cnx.org/contents/f443169d-16c3-402f-9712-17a994953365@2/differential-scanning-calorimetry-dsc>]

General DSC curve is shown in figure 11. Some machines give exothermal heat as negative heat and some machines generate exothermal heat as positive heat. In this graph, heat released is positive. Oxidation processes are always exothermic while pyrolysis processes are often endothermic.

Chapter 5. Fuel Analysis

To know about characteristics of fuel, knowledge of fuel composition is necessary. For that, proximate and ultimate analysis of fuel is carried out. Proximate analysis was done using TG characteristic graphs and ultimate analysis is done using gas chromatography of flue gas from fuel.

5.1 Proximate analysis

Initially pyrolysis of dried dung cake is done using Nitrogen at 20 °C/min from 40°C to 800°C in TA Instruments SDT 2960, instrument used for TG analysis. As the fuel quantity used in equipment was around 10 milligrams and that content of fuel can be non-homogeneous in nature, for that five reproducibility experiments were done. TG curves of five experiments are shown in figure 12. In the beginning, from 40°C to 200°C, a slight decrease of mass is observed which corresponds to the total moisture content in the fuel is. [42] Later on, after 200°C all the volatile matter in fuel is released and at the end of pyrolysis only charcoal is left.

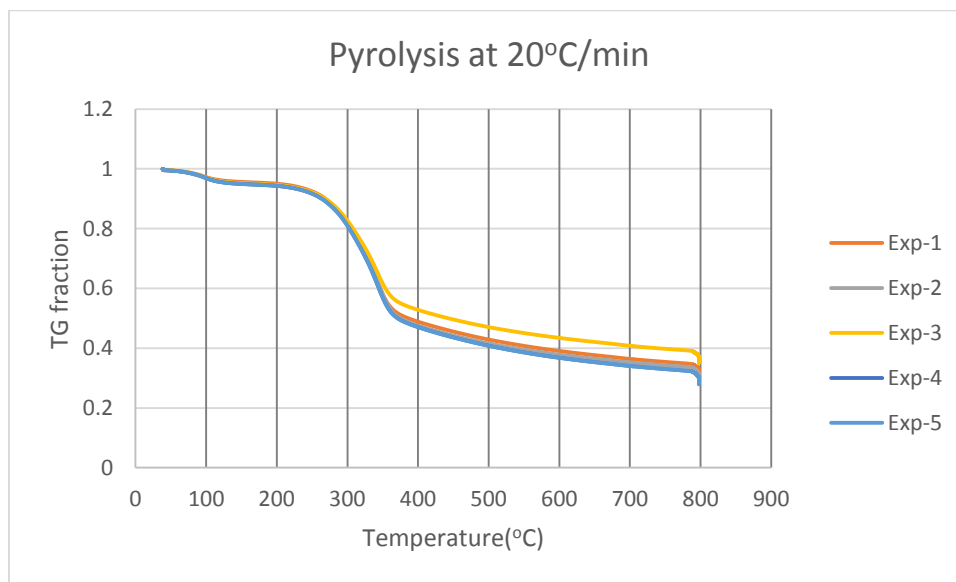


Figure 12 TG curves of Pyrolysis of Dung Cake.

After pyrolysis, combustion of charcoal is done using the same cycle used for pyrolysis, but using air as the flow gas, and TG curve for combustion is obtained which is shown in figure 13. At the end of combustion of charcoal only ashes are left behind. So, by using simultaneously the pyrolysis and combustion data, the moisture, volatile matter, fixed carbon and ash content is obtained.

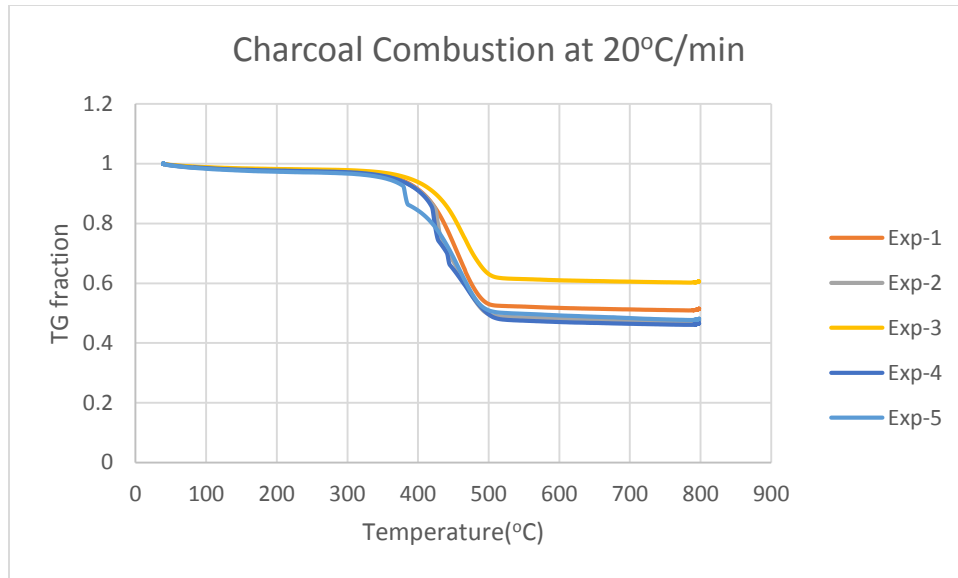


Figure 13 TG curve of combustion of charcoal

Result of five experiments are shown in table 5.

Table 5 Proximate Analysis of Dung cake.

No. of experiment	1	2	3	4	5	Standard Deviation	Average values
Initial mass(mg)	10.04	10.01	9.98	9.94	10.48		
Mass after 200°C(mg)	9.58	9.48	9.49	9.42	9.93		
Mass after Pyrolysis(mg)	3.08	2.90	3.49	2.77	2.92		
Mass after Combustion(mg)	1.66	1.50	2.17	1.41	1.51		
Moisture (%)	4.48	5.18	4.88	5.15	5.22	0.28	5.01
Volatile Matter (%)	64.81	65.80	60.14	66.91	66.92	2.51	66.11
Fixed Carbon (%)	14.10	14.01	13.17	13.73	13.47	0.34	13.83
Ash (%)	16.59	15.01	21.78	14.18	14.38	2.83	15.04
Total	100	100	100	100	100		100

From the standard deviation, it is observed that experiment 3 has deviating result from rest of the experiments. So, to calculate the average values of moisture, volatile matter, fixed carbon and ash content, values are only considered from experiment 1, 2, 4 and 5 which are almost constant. Following formulas are used to find out respective content of entities.

$$\text{Moisture } (M)(\%) = \frac{\text{Initial mass} - \text{Mass after } 200^\circ\text{C}}{\text{Initial mass}} * 100 \quad (5.1)$$

$$\text{Volatile Matter (VM)(\%)} = \frac{\text{Mass after 200 }^\circ\text{C} - \text{Mass after Pyrolysis}}{\text{Initial mass}} * 100 \quad (5.2)$$

$$\text{Fixed Carbon (FC)(\%)} = \frac{\text{Mass after Pyrolysis} - \text{Mass after Combustion}}{\text{Initial mass}} * 100 \quad (5.3)$$

$$\text{Ash (A)(\%)} = 100 - (M + VM + FC) \quad (5.4)$$

Average results of proximate analysis of dung cake are also shown in table 5. This method is not a standard method. It is performed to have an approximate measurement of all the relevant quantities of proximate analysis.

5.2 Ultimate analysis

Ultimate analysis is elemental analysis of fuel. It was carried out in Analysis Laboratory of IST, Lisbon (LAIST) using their indigenous methodology M.M. 8.6 (A.E) (2009-05-06) and using Fisons Instrument EA 1108 instrument. First, the fuel is combusted and then amounts of C, H, N and S are analyzed using gas chromatography of flue gases. Analysis was performed three times and average of the three values are taken as final result. Result of the ultimate analysis is shown in table 6.

Table 6 Ultimate Analysis of Dung cake

	As Received(%)
N	1.57
C	38.95
H	5.05
O	34.36
S	<2%
Moisture	5.01
Ash	15.04
HCV^a(kJ/kg)	15.65
LCV^a(kJ/kg)	14.31

*a = dry basis

Results obtained are of as received basis. C, H, N and S were obtained from the analyzer; moisture and ash content were obtained from proximate analysis. Oxygen content is found by difference as mentioned in equation (1.1). Exact value of Sulphur content is not shown because the machine has sensitivity to Sulphur only if it is more than 2%. HCV on dry basis is calculated from the Channiwala and Parikh equation [23] shown in equation (1.2). LCV of the fuel is obtained by equation (1.3). Obtained fuel ultimate and proximate analysis is similar to the rice husk fuel analysis, both are having high ash and high volatile content [24]. Also, as it can be seen the moisture and ash contents obtained by the two different analysis and in good accordance with each other.

Chapter 6. Thermal Analysis of Dried Dung

6.1 Sample Preparation

Dung cakes, which were used for thermal analysis, are shown in figure 14. They were collected from site and dried in heat of Sun. When dry, the cakes are collected and used as fuel.



Figure 14 Dung cakes used in experiment

As in TGA and DSC analysis the sample is used in very small quantities the cakes have to be ground to fine particles. Dung cake was ground using mortar and pestle until it was fine grain.

6.2 Equipment

TA Instruments SDT 2960 Simultaneous DSC-TGA

Equipment contains a standard furnace, which can be heated 1500° C. However, the highest temperature that samples were heated, is to avoid burnout of the furnace. The heating rates used ranged from 0.1 °C/min to 100 °C/min. A cooling of the crucibles used for experiment is done by instrument air which is forced inside the furnace. Aluminum oxide crucibles were used for loading the samples. An image of the equipment is presented in figure 15. The equipment is linked to a computer installed with TA Instruments software, which was used to control the equipment and display the results of the experiments.



Figure 15 TA Instruments SDT 2960 Simultaneous DSC-TGA

Simultaneous DSC-TGA measures both the heat flows (DSC) and weight changes (TGA) associated with transitions in a material as a function of temperature and time in a controlled atmosphere.

6.3 Pyrolysis

Procedure

Initially, around 10 mg of sample is placed into an alumina pan which was mounted in the thermal analysis equipment, which has been tared for the weight of the pan itself. For pyrolysis, four experiments, with combination of char combustion at the end of pyrolysis, were done. Programming of the experiment is shown in below table 7.

Table 7 Programming for Pyrolysis Experiment

No	Pyrolysis				Combustion			
	Initial Temperature (°C)	Final Temperature (°C)	Isothermal at 800 °C (min)	Heat Rate (°C/min)	Initial Temperature (°C)	Final Temperature (°C)	Isothermal at 800 °C (min)	Heat Rate (°C/min)
1	40	800	10	5	40	800	30	20
2	40	800	60	20	40	800	30	20
3	40	800	60	50	40	800	30	20
4	40	800	60	100	40	800	30	20

Pyrolysis was done at four different heating rates 5, 20, 50, 100 °C/min, from an initial temperature of 40 °C to 800 °C. The sample is maintained at 800 °C for 60 minutes for higher heating rates and 10 minutes for lower heating rates. Char combustion after every pyrolysis experiment was always done under the same conditions i.e. heat rate 20 °C/min and isothermal for 30 minutes at 800 °C. For inert medium in furnace, nitrogen is used at constant flow rate of 50 ml/min and for combustion, air is used at 50 ml/min for all the experiments done.

Kinetic Analysis

From figure 16, it can be noticed that there are three stages of mass loss, the first one from 40 °C to 200 °C, the second from 200 °C to 350 °C and third in the end till 800 °C. This indicates that there are three types of materials or processes in the sample. The first stage can be explained by presence of moisture that evaporates till the sample reaches 200 °C.

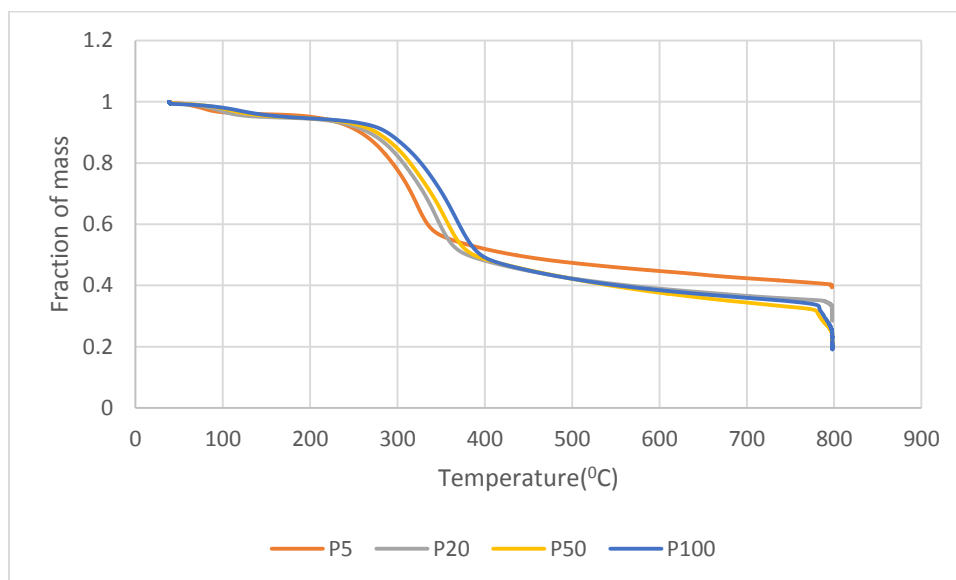


Figure 16 Pyrolysis of dung cake at different heat rate.

As dung cakes are lignocellulosic materials, the second and third stage is the decomposition of these materials present in the sample. The second stage can be associated with the presence of cellulose and hemicellulose and third stage can be explained by the presence of lignin [45].

Effect of heating rate on volatile matter (VM) produced during pyrolysis

The effect of heating rate on char production was studied by S. Katyal. Heating rate influences the rate of volatile evolution from the biomass. The higher heating rate above 400°C promotes rapid volatile evolution. The molecular disruption is extremely fast and volatile fragments are released so rapidly that successive adjustments and equilibrium leading to further primary reactions that yield char have less opportunity to

take place [46] This effect can be seen in figure 17. As the heat rate increases amount of volatiles released increases.

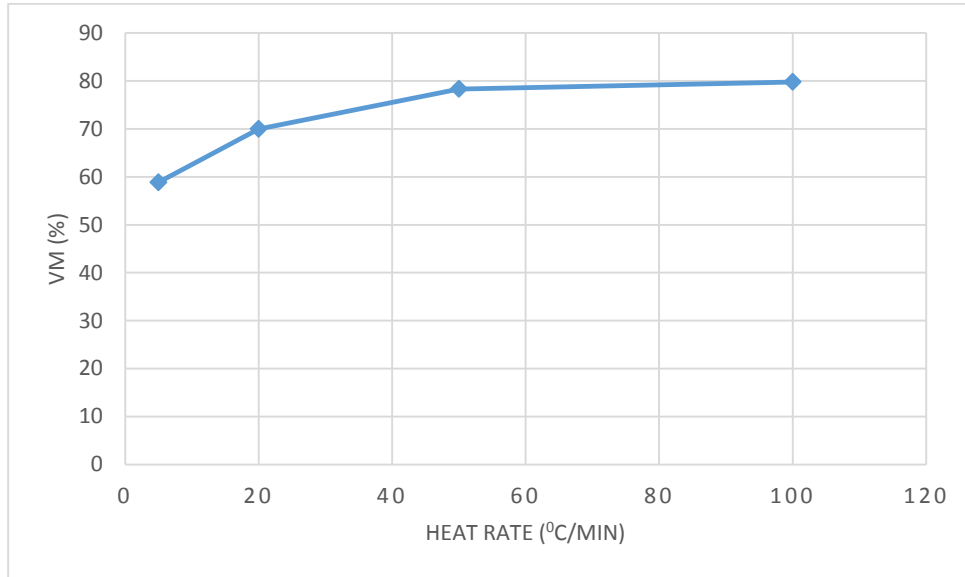


Figure 17 Effect of heat rate on volatiles produced

DSC curves of dung cake are shown in figure 18 with exothermic values as positive. Initial peak in the region between 40 °C and 200 °C is due to moisture evaporation which is an endothermic reaction. Heat released during pyrolysis of biomass can be explained by decomposition of the Lignocellulosic structure of biomass. At higher temperatures (above 500 °C) , polysaccharides compounds in cellulose and hemicellulose undergo fission, dehydration, disproportionation and decarboxylation reactions to provide a mixture of low molecular weight gaseous and volatile products. It can be seen that the pyrolysis processes seem to be slightly endothermic at relatively low heating rates but, as the heating rate is increased from 5 to 100 °C/min, the process becomes exothermal.

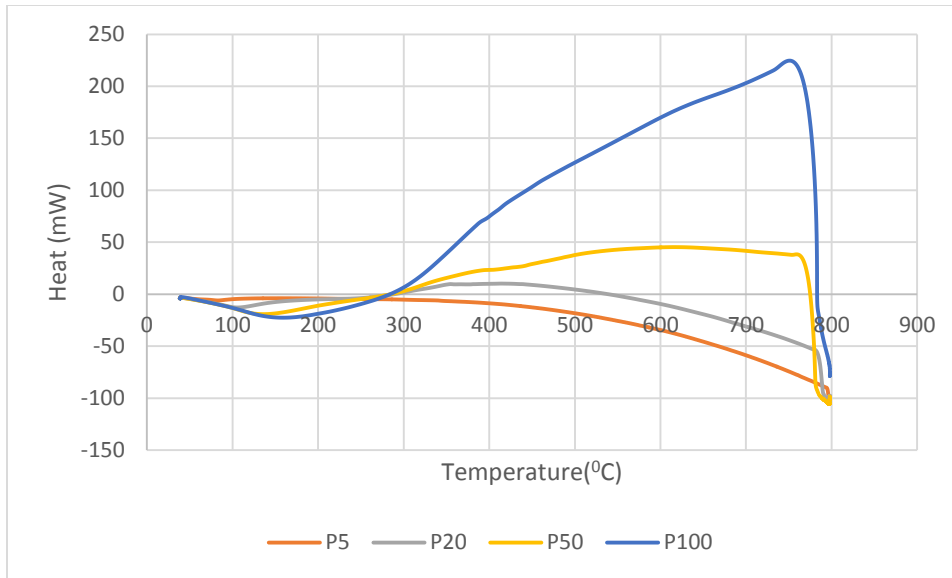


Figure 18 DSC curves of dung cake pyrolysis at different heat rates

Effect of heat rate on char produced during pyrolysis

The amount of char produced after each pyrolysis process is found out by combustion of char because char produced contains generally two entities, fixed carbon and ash. Only Char is combustible, so in the end of combustion operation ash will be left. The relationship between the amount of char produced and the heating rate of the pyrolysis operation is shown in figure 19.

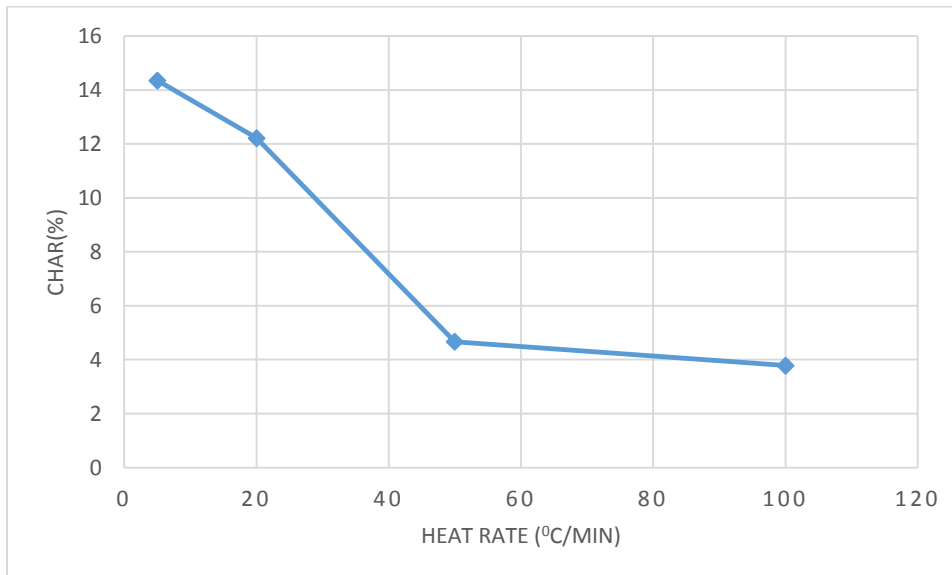


Figure 19 Effect of heat rate on char produced.

As it is seen that with increase in heat rate, amount of char produced after pyrolysis decreases. This result can also be observed on the DSC curves corresponding to the combustion of the char produced, which is presented in Figure 20. As, the quantity of char increases, the amount of heat released during the combustion process also increase.

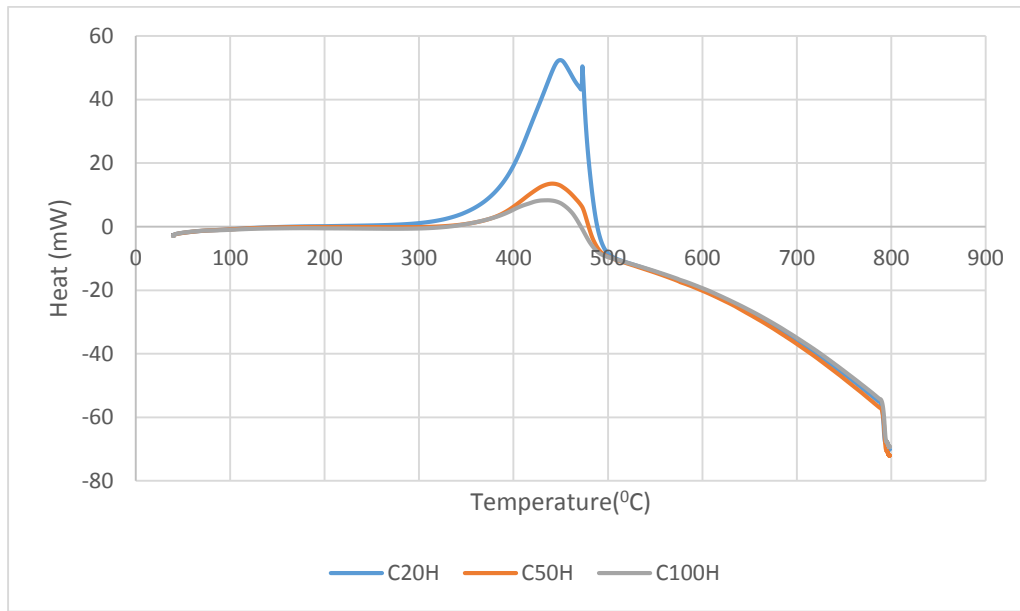


Figure 20 DSC curves of combustion of char

Char Characteristics

Char is a high calorific value product of pyrolysis that contains a high amount of carbon. For the combustion analysis the data from pyrolysis at 5 °C/min is taken as it produced the highest amount of char. A graph of the derivative of the weight (mg/min) vs temperature is shown in figure 21.

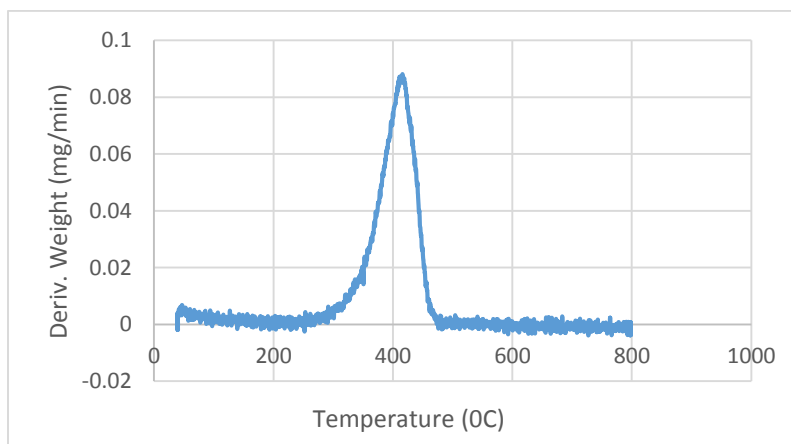


Figure 21 DTG curve for the combustion of the char produced for the pyrolysis experiment at 5 °C/min.

The most important characteristic temperatures of a combustion profile are the ignition temperature and the peak temperature. The ignition temperature corresponds to the point at which the burning profile undergoes a sudden rise. The ignition temperatures of samples are determined from their burning profiles. The point on the burning profile at which is the rate of weight loss due to combustion is maximum is known as peak temperature [48]. In the case the ignition temperature of char derived from dung cake is around 300 °C and the peak temperature is around 420 °C.

6.4 Combustion

Procedure

Around 10 mg (roughly measured) of the sample is placed in an alumina pan and set in the thermogravimetric apparatus. The equipment was tared with the empty pan and then programming for the experiment in equipment is started. For combustion, four experiments with different heat rates are done. Programming for the combustion experiment is shown in table 8. Air flow in the furnace is 50 ml/min and it is maintained constant for all the experiments.

Table 8 Programming for combustion experiments

Combustion				
No.	Initial Temperature (°C)	Final Temperature (°C)	Isothermal at 800 °C (min)	Heat Rate (°C/min)
1	40	800	10	5
2	40	800	60	20
3	40	800	60	50
4	40	800	60	100

Kinetic Analysis:

The kinetics of the combustion of biomass was studied, for example, by Haykırı-Açma Hanzade. [49]. When biomass is combusted in the beginning moisture is released. Then combustion of volatile matter and carbonization of fixed carbon occurs and then combustion of carbonized char occurs. This three phenomena can be observed from the DTG curves [49].

As already discussed, to study combustion of biomass DTG curves are useful. The DTG curve of combustion of dung cake at 5 °C/min heating rate is shown in figure 22. In this figure, three different peaks are visible. In the beginning, first peak of mass loss shows evaporation of moisture. The second peak corresponds to the combustion of volatile matter which starts at 180 °C and ends at 400 °C. Third peak between 430 °C to 500 °C shows combustion of carbonized char.

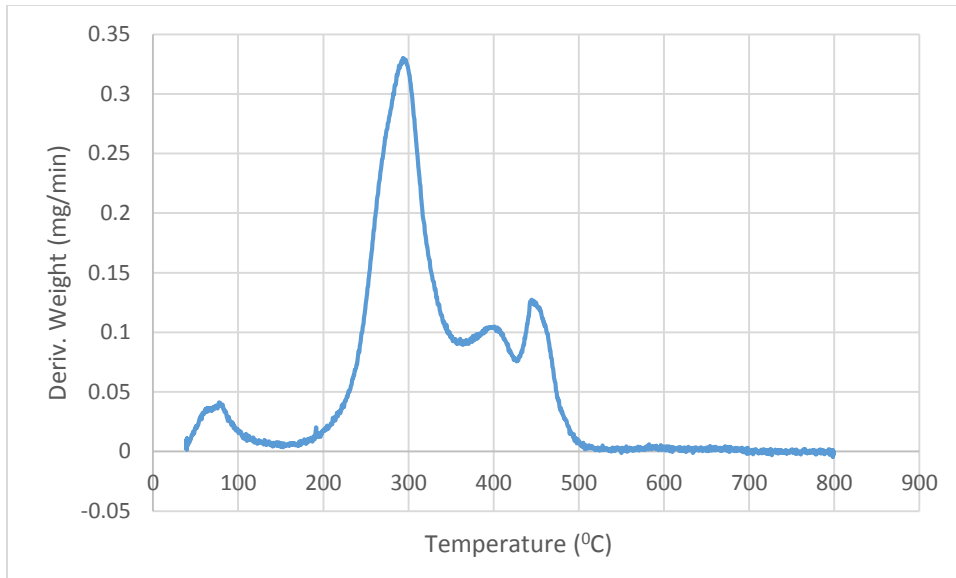


Figure 22 DTG curve of combustion of dung cake

To verify whether the process is combustion or not, DSC curves of combustion and pyrolysis are compared in figure 23. As seen from figure, in the beginning, both curve follows same path. After 250 °C, combustion curve becomes exothermic. Also, comparing both the curves, heat released during combustion process is way higher compared to pyrolysis.

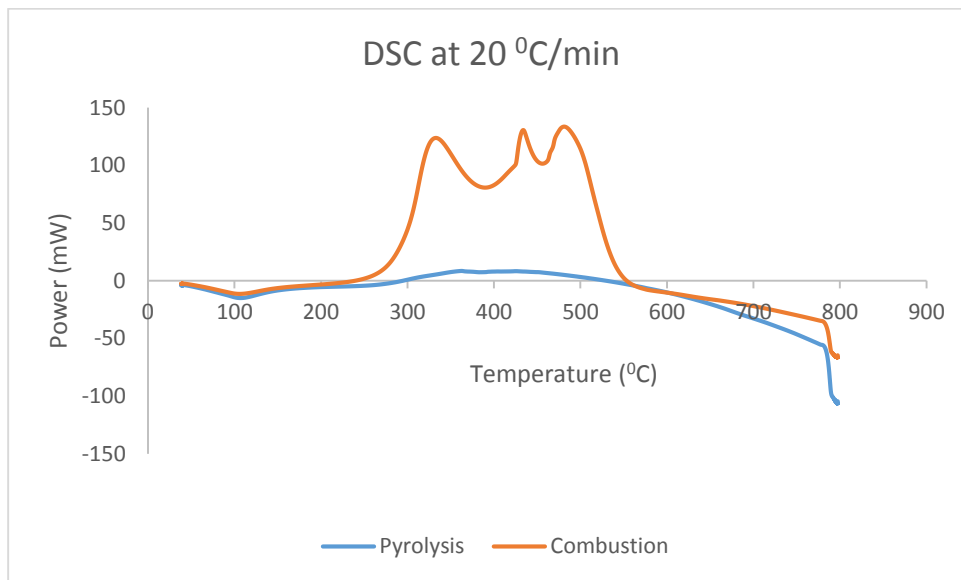


Figure 23 Comparison of DSC curves of combustion and pyrolysis

The heating rate was increased from 5 °C/min to 100 °C/min. From figure 24, it can be seen that, as heating rate increases, the ignition temperature, peak combustion rate and peak temperature increases. The rate

of weight loss at the peak temperature in the combustion profile is called the maximum combustion rate. Also, carbonized char content decreases as the heat rate increases. That is the reason that third peak in combustion at 100 °C/min is very low.

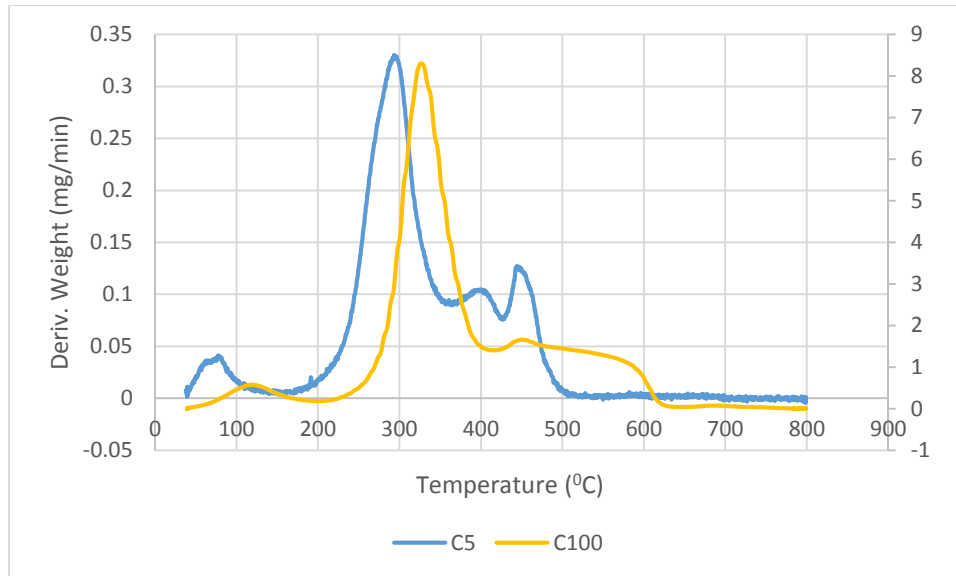


Figure 24 DTG curves at different heat rates

Ignition temperature, peak combustion rate and peak temperature at different heat rates 5, 20, 50, 100 °C/min is tabulated in table 9.

Table 9 Effect of heat rate on combustion parameters

Heat rate (°C/min)	Ignition Temperature (°C)	Peak Temperature (°C)	Peak Combustion Rate (mg/min)
5	180	291	0.3
20	192	320	1.52
50	201	324	5.06
100	214	332	8.24

6.5 Influence of Oxygen Partial Pressure (Partial Oxidation)

Procedure

Initially, around 10 mg of sample is placed in an alumina pan that is set in thermogravimetric apparatus. The equipment was tared with an empty pan and then the programming for the experiment in the equipment is started. For partial combustion, six experiments with same heat rate and different oxygen content are done. The programming for the combustion experiments is shown in table 10. For partial oxidation, air flow is varied from the one used in the previous complete combustion experiments (50 ml/min of air) to pyrolysis

conditions (no air). Total flow in the furnace is 50 ml/min and it is maintained constant for all the experiments; nitrogen was used as make-up gas. In number coding, C50 means partial oxidation at 50 ml/min air flow.

Table 10 Programming for partial oxidation

No.	Initial Temperature (°C)	Final Temperature (°C)	Isothermal at 800 °C (min)	Heat Rate (°C/min)	Oxygen Flow (ml/min)	Nitrogen Flow (ml/min)	Total Flow (ml/min)
C50	40	800	10	5	10.5	39.5	50
C25	40	800	10	5	5.25	44.75	50
C12.5	40	800	10	5	2.625	47.375	50
C5	40	800	10	5	1.05	48.95	50
C2.5	40	800	10	5	0.525	49.475	50
C0	40	800	10	5	0	50	50

Kinetic Analysis

Kinetic study of partial oxidation of lignocellulosic biomass was studied by Amutio Maider et al. As oxygen supplied to biomass decreases during different oxidation experiments, ignition temperature, peak temperature increases and peak combustion rate decreases [50].

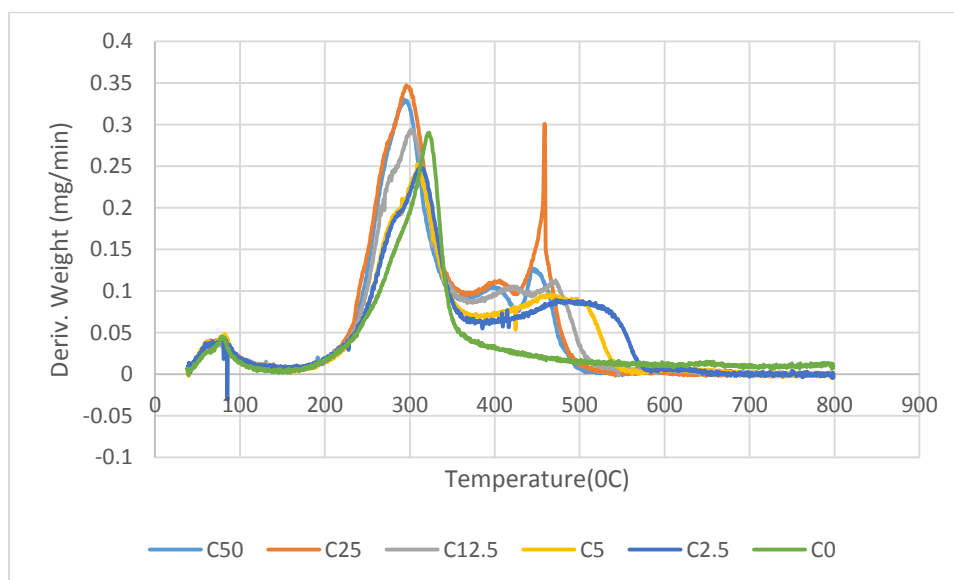


Figure 25 DTG curves of partial oxidation of dung cake.

As it is noticeable from figure 25, as amount of oxygen decreases, third peak is getting flatter. This means that the amount of fixed carbon that was burning during higher air supply is now converted into char. From table 11 is visible that as air supply decreases ignition temperature and peak temperature increases and peak combustion rate decreases. As the air flow decreases, char combustion rate decreases and maximum

char combustion temperature increases. It can be seen in figure 25 that by decrease in air content, third peak moves rightwards and when there is no air (pyrolysis), it disappears.

Table 11 Combustion characteristics with change in oxygen flow

No.	Ignition Temperature(°C)	Peak Temperature(°C)	Peak Combustion Rate (mg/min)	Max. char combustion Temperature (°C)
C50	173	298	0.32	451
C25	181	299	0.34	459
C12.5	184	304	0.29	471
C5	187	311	0.25	478
C2.5	191	314	0.24	496
C0	185	323	0.28	-

DSC curves of the partial oxidation of dung cake at different air supply rates are shown in figure 26. Graph is between heat supplied/released (mW) to time (min), so the area under the curve indicates the total amount of heat released during the oxidation process. In the figure 26 we can see clearly two peaks, apart from the drying at very low temperatures; the first corresponds to the combustion of volatiles and second being combustion of char. As, the oxygen partial pressure decreases, the amount of heat released decreases.

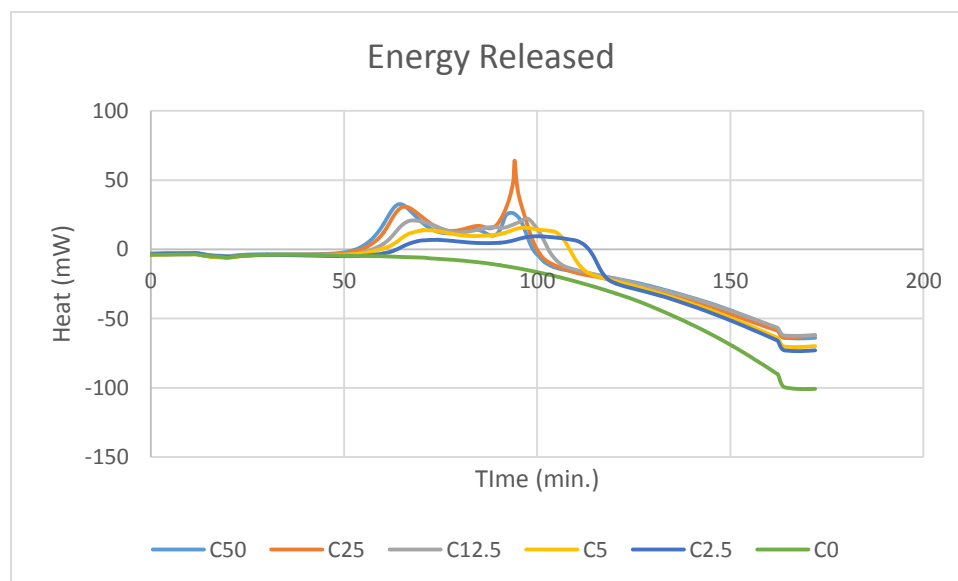


Figure 26 DSC curves of partial oxidation of dung cake.

Chapter 7. Kinetic Modelling of Thermochemical Processes

7.1 Introduction

Before considering kinetic model for dried cattle dung thermochemical conversion, pathway of reaction process must be studied in order to determine either volatile material or heterogeneous reaction influences the process. The identification of the kinetic pathway can be carried out by analyzing the shape of the DTG curve for solid fuel oxidation and comparing it with the curve for pyrolysis [54]. Figure 26 shows the DTG curves for the pyrolysis and oxidation of pinewood sawdust, with 0, 5, 10 and 20 vol. % of oxygen performed by Amutio Maider, et al [50].

As it can be seen in figure 27, biomass oxidation has two peaks, the first peak is shifted to lower temperatures than that corresponding to pyrolysis as the oxygen content increases and the second peak at higher temperatures is related to char combustion, as it has been observed in section 6.5 of the report. This shape evidences a synergistic effect of purely thermal degradation and heterogeneous oxidation, occurring over comparable time scales [50].

The shape and position of both peaks in Figure 27 depend on the amount of oxygen supplied. At higher oxygen concentrations, both peaks appear at lower temperatures, and the peak corresponding to the combustion of char becomes sharper as observed in section 6.5.

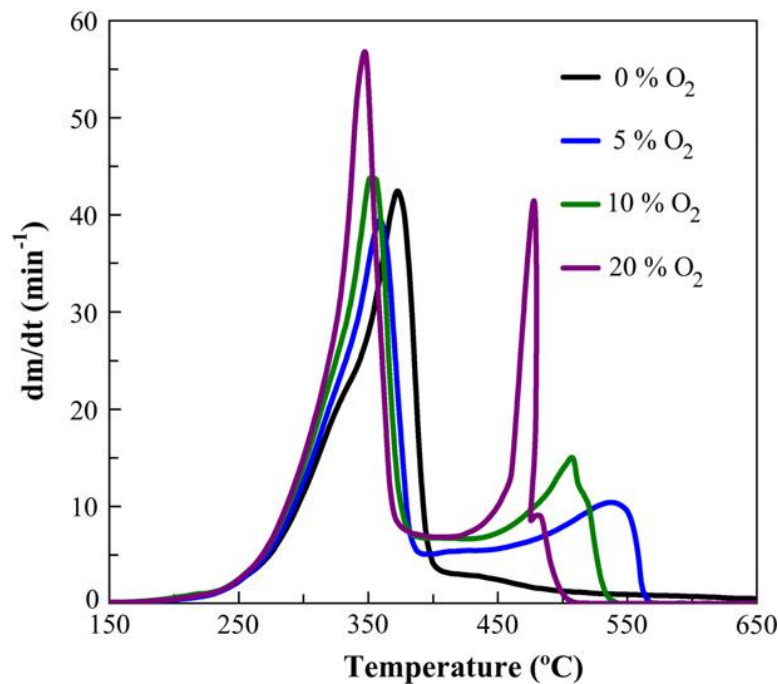


Figure 27 Comparison of Pyrolysis and oxidation of lignocellulosic biomass [50]

Lignocellulosic biomass is made up of three main components: hemicellulose, cellulose and lignin, which in the case of dry ash free cattle dung correspond approximately to 23.8, 32.6 and 26.8 wt. %, respectively [51], and lower amounts of extractives. Amutio, Maider, et al. has studied oxidation of pine sawdust and three components of ligno cellulosic materials; xylan (hemicellulose), cellulose and lignin. As shown in figure 28, biomass oxidizes in a wide temperature range, where the decomposition of the three biomass components overlaps. [50]

A thermo-gravimetric study was performed by Amutio, Maider, et al. [50] using xylan, cellulose and lignin as reactants, shown in figure 28. As observed, the oxidative pyrolysis of the three main components of biomass gives way to two main peaks. The first one (at lower temperature) corresponds to the pyrolysis and heterogeneous oxidation whereas the second one is attributed to the combustion of char.

Xylan or hemicellulose is the component with the lowest thermal stability, and both peaks appear at the lowest temperatures (270 and 410 °C). Cellulose decomposes in a narrow peak at 320 °C and the peak corresponding to char combustion is wide and low. Finally, lignin volatilizes in a wide range of temperatures, resulting in a high char yield, which burns at the highest temperature (around 560 °C) [50]. So, from this, we can conclude that cellulose and hemicellulose are the two main components of volatile matter and lignin composition signifies the amount of char.

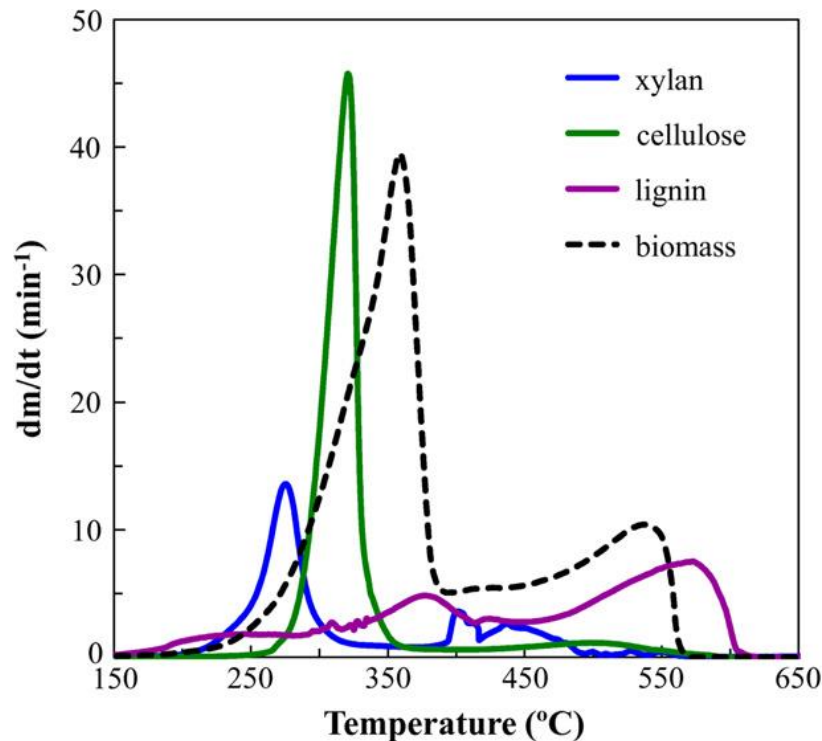


Figure 28 DTG curves of partial oxidation of pinewood, xylan, cellulose and lignin at $PO_2 = 0.05$ atm. [30]

7.2 Euler's method

In this kinetic model, to solve first order differential equation, Euler's method is used. Random first order differential equation with initial conditions can be written as

$$\frac{dy}{dt} = f(t, y), \quad y(t_0) = y_0 \quad (7.1)$$

Now, to find value of y at time t_1 , Euler's method uses a linear model, that is shown in figure 29. Tangent line represents the linear model to find out the value of y at time t_1 .

$$y = y_0 + f(t_0, y_0) * (t - t_0) \quad (7.2)$$

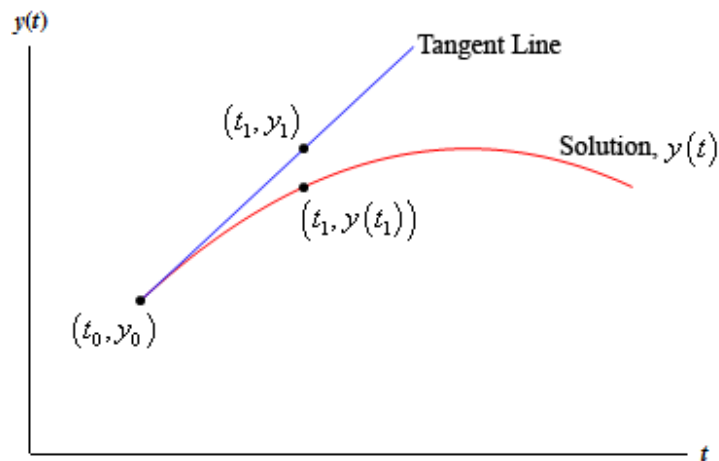


Figure 29 Euler's Method

(Source: <http://tutorial.math.lamar.edu/Classes/DE/EulersMethod.aspx>)

Euler's method gives approximate results and there are errors associated with it. But these errors can be reduced by taking, as much as possible, a small time interval.

7.3 Langmuir Adsorption

For partial oxidation Langmuir's adsorption theory is used for modelling. An analysis into surface reactions in gasification and pyrolysis can be beneficial from looking into surface reactions involved in heterogeneous catalysis [55].

The Langmuir adsorption model explains adsorption by assuming an adsorbate behaves as an ideal gas at isothermal conditions. At these conditions the adsorbate's partial pressure (p_A), is related to the volume (V) adsorbed onto a solid adsorbent. [56] The adsorbent is assumed to be an ideal solid surface composed of series of distinct sites capable of binding the adsorbate. The adsorbate binding is treated as a chemical reaction between the adsorbate molecule (A_g) and an empty site (S). This reaction yields an adsorbed complex (A_{ad}) with an associated equilibrium constant (K_{eq}).



The rate of this reaction depends on the magnitude of the adsorption coefficient (K_{eq}), which is the equilibrium constant for the reaction defined by the ratio of the rate constant of adsorption to rate constant of desorption. The rate of surface reactions is also limited by the number of available surface sites. [55] From these assumptions the Langmuir isotherm can be derived, which equates to:

$$\theta_A = \frac{V}{V_m} = \frac{K_{eq} * p_A}{1 + K_{eq} * p_A} \quad (7.3)$$

Where, θ_A is the fractional occupancy of the adsorption sites and V_m is the volume of the monolayer. A continuous monolayer of adsorbate molecules surrounding a homogeneous solid surface is the conceptual basis for this adsorption model. [56]

The Freundlich isotherm is the most important multisite adsorption isotherm for rough surfaces which is equated below:

$$\theta_A = \alpha_F * p^{C_F} \quad (7.4)$$

Where, α_F and C_F are fitting parameters. This equation implies that if one makes a log-log plot of adsorption data, the data will fit a straight line. The Freundlich isotherm has two parameters while Langmuir's equations has only one. Which concludes that it often fits the data on rough surfaces better than the Langmuir's equations. Rearranging the Langmuir equation, one can obtain: [57]

$$\theta_A = \frac{p_A}{\frac{1}{K_{eq}} + p_A} \quad (7.5)$$

Equation (7.5) is further used in modelling of kinetic parameters of partial oxidation.

7.4 Kinetic Model for Pyrolysis

As discussed earlier, during pyrolysis process all the moisture and volatile matter in the fuel sample evaporates and in the end only char and ash remain [50].

From figure 28, we can see that the three major components of lignocellulosic biomass: hemicellulose, cellulose and lignin, have significant roles in the pyrolysis of the biomass sample. Cellulose and hemicellulose contains high amount of volatile matter and very low fixed carbon and lignin contains very low volatile matter and high amount of fixed carbon. This simplifies pyrolysis of lignocellulosic materials.

For kinetic modelling, pseudo component modelling method is used [52]. Total material mass at any time in process is divided between four pseudo components of biomass; moisture, hemicellulose; cellulose, lignin. Ash is the residual component which remains fixed always. During pyrolysis process, part of lignocellulose that gets converted to char is also accounted into ash while modelling.

Equations related to modelling

Before starting the model a short discussion of the equations used is necessary. The Arrhenius equation, shown in equation (3.4), was used for all kinetic rate constants

$$k = A e^{\frac{-E_a}{RT}}$$

In this equation terms which are temperature dependent are rate constant k. Frequency factor A, activation energy E_a and universal gas constant R do not vary much with respect to change in temperature.

Imagine, if we want to measure rate constant and activation energy at temperature $T_0 = 300$ °C (573 K) then value of k will change. Considering T at 300 °C as reference value then value of temperature and rate constant at reference value would be T_{ref} and k_{ref} and equation (3.4) can be modified as:

$$k_{ref} = A * e^{\frac{-E_a}{R * T_{ref}}} \quad (7.6)$$

Now, dividing equation (3.4) by Equation (7.6) and after simplification we get,

$$k(T) = k_{ref} * e^{\frac{-E_a}{R} [\frac{1}{T} - \frac{1}{T_{ref}}]} \quad (7.7)$$

This was the form that was used for the application of the Arrhenius equation because it reduces correlation between the activation energy and the pre-exponential coefficient during the fitting.

Considering all the reactions occurring with pseudo components as first order reactions, rate of reaction can be written as,

$$\frac{dW}{dt} = k(T) * W \quad (7.8)$$

Where, W is the weight of pseudo component at time t and $k(T)$ is rate constant at temperature T . Now, quantity of pseudo component at any time can be found out by using Euler's method for solution of first order differential equation. Therefore, quantity of pseudo component at time t can be written as,

$$W_1 = W_0 + \frac{dW}{dt} * (t - t_0) \quad (7.9)$$

Where W_0 is the weight of sample at time t_0 . Time step $(t - t_0)$ is 0.001 second. Equation (7.7), (7.8) and (7.9) are used extensively in kinetic modelling.

Model

Initially thermo gravimetric analysis was performed on dung cake at different heat rates (5, 20, 50, 100 °C/min) with nitrogen as mentioned in section 6.3. For pseudo component model, each component (moisture, hemicellulose; cellulose, lignin) was assigned an initial value (later on taken as variable value subject to fitting) and using equation (7.7) their rate constants were found at any time t . After finding rate constant rate of each pseudo component was found out by using equation (7.8). From rate of reaction, pseudo weight was found out by using equation (7.9). At any time t , summation of mass of all pseudo component with the mass of ash will give an estimate of the amount of matter left in pan in analyzer at any time t . Total modelled weight W_{model} of sample at any time t during process will, thus, be,

$$W_{moi} + W_{hemi} + W_{cell} + W_{lig} + W_{ash} = W_{model} \quad (7.10)$$

Where, W_{moi} is moisture content, W_{hemi} is hemicellulose content, W_{cell} is cellulose content, W_{lig} is lignin content, W_{ash} is ash content, and W_{model} is total weight of sample at any time t .

Modelling is done using excel solver program. In which first objective function has to be set up. In this model objective function is taken as summation of square of error (difference of practical weight $W_{practical}$ and modelled weight) at different heat rates. Objective function is shown as,

$$O.F. = \sum_{i=1}^4 * \sum_{j=1}^N (W_{practical} - W_{model})^2 \quad (7.11)$$

Where, $j = 1, 2, \dots, N$ is the total no. of steps in the experiments and $j=1, 2, 3$ and 4 are values of total square of error at heat rates of $5, 20, 50$ and 100 °C/min respectively.

The quality of curve fitting is evaluated by [58],

$$Fit (\%) = \left(1 - \frac{\sqrt{\frac{O.F.}{N}}}{[(W)_{Practical}]_{max}} \right) * 100 \quad (7.12)$$

Where, N is total no. of steps in the experiment,

In a nutshell the total process of modelling can be viewed in figure 30 as shown below. First four pseudo component's rate constant at T_{ref} (k_0), activation energy E_a and initial weight W_0 of each component is assumed. For all the four heat rate variations ($5, 20, 50$ and 100 °C/min), rate constant at T_{ref} and activation energy of each pseudo component is taken as same. As modelling is done based on weight, composition of each pseudo component may vary in each heat rate variation experiment. Also, as discussed in section 6.3, pyrolysis process' composition depends upon the heat rate applied during pyrolysis process. So, it is better to have different composition for all the pseudo components for different experiment value.

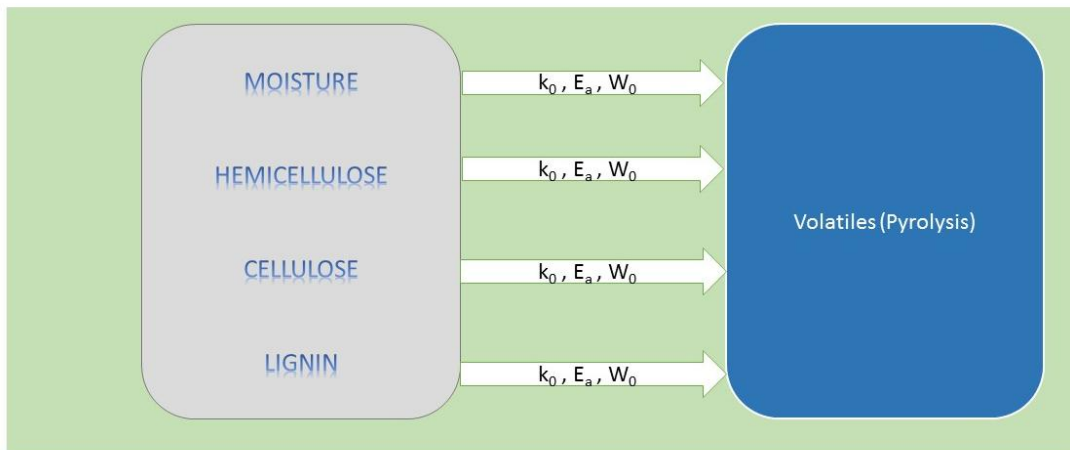


Figure 30 Mechanism of the kinetic modelling of pyrolysis

So, in excel solver program k_0 , E_a and component wise W_0 are taken as variables subject to fitting and the sum of the squares of errors is taken as objective function. After numerous solving iterations, results were found which are discussed below.

Results

Here, overall composition based on model that was used for pyrolysis is shown in table 12. As, we can see from hemicellulose and cellulose content, both decrease with increase in heat rate; which explains that volatilization is higher at high heat rates and vice versa. Estimated lignin content does not vary much by varying heat rates. Whereas, ash content is higher at low heat rates and decreases with increase in heat rate. It is to be reminded that here ash contains mixture of charcoal and mineral matter. Mineral matter does not vary much from sample to sample. So, the variable in this content is charcoal only. This phenomenon is explained in section 6.3 in *Effect of heat rate on volatile matter (VM) produced during pyrolysis*. Moisture content does not vary much with heat rates as the chemistry is about evaporation of moisture into vapor.

Total volatile matter evaporated from experiments and from model are compared in table 12. Experimental (practical) values of volatile matter are derived from TG curves. Model values are the summation of hemicellulose, cellulose and lignin. From the comparison it is noticed that the values are similar and it is in range of error of 0.06 – 1%.

Table 12 Composition of lignocellulosic material in pyrolysis at different heat rates

Composition	Hemicellulose (%)	Cellulose (%)	Lignin (%)	Ash* (%)	Moisture (%)	VM (%)	
						Model	Practical
P5	6.57	32.85	16.87	39.14	4.56	56.29	56.07
P20	8.94	41.15	16.01	28.46	5.44	66.10	66.84
P50	8.74	47.12	18.02	20.52	5.60	73.88	73.45
P100	8.90	48.21	17.97	19.15	5.76	75.08	75.13

***ash contains char and mineral matter**

Part of the differences observed in the composition estimated for the samples in the different experiments can be justified by the intrinsic variability of the samples, as they are composed of biological material and are relatively small, but part can also be associated with modelling errors due to the assumption that were made and can probably be further reduced by increasing the complexity of the model. The activation energies for the pyrolysis of the different pseudo components are shown in table 13. From the experiments of J. J. Orfão et al. of pyrolysis of different components of lignocellulosic biomass it can be concluded that while pyrolyzing biomass initially moisture evaporates followed by destruction of hemicellulose, cellulose and lignin structure destruction [52].

Table 13 Activation energies estimated for the pyrolysis of the different pseudo components considered.

	Hemicellulose	Cellulose	Lignin	Moisture
k(300) (1/min)	0.62	0.07	0.01	22.48
Ea (kcal/mol)	18.04	24.98	5.53	9.46

High values of $k(300)$ and activation energy E_a suggests that hemicellulose will decompose at lower temperatures and lower values of $k(300)$ and E_a suggests that lignin will decompose in wide range of temperature. Whereas, cellulose will have higher peak because of high value of E_a and decompose after hemicellulose because of lower value of $k(300)$. This can be observed from the differential curves obtained during modelling, shown in figure 31. As observed from figure, initially moisture evaporates followed by the degradation of hemicellulose, cellulose and lignin with cellulose having high steep peak.

The activation energy for moisture evaporation should be close to the latent heat of evaporation of water. In fact the estimated values obtained from modelling are around 9.47 kcal/mol, which is a value that is very near to literature value of 9.67 kcal/mol [59].

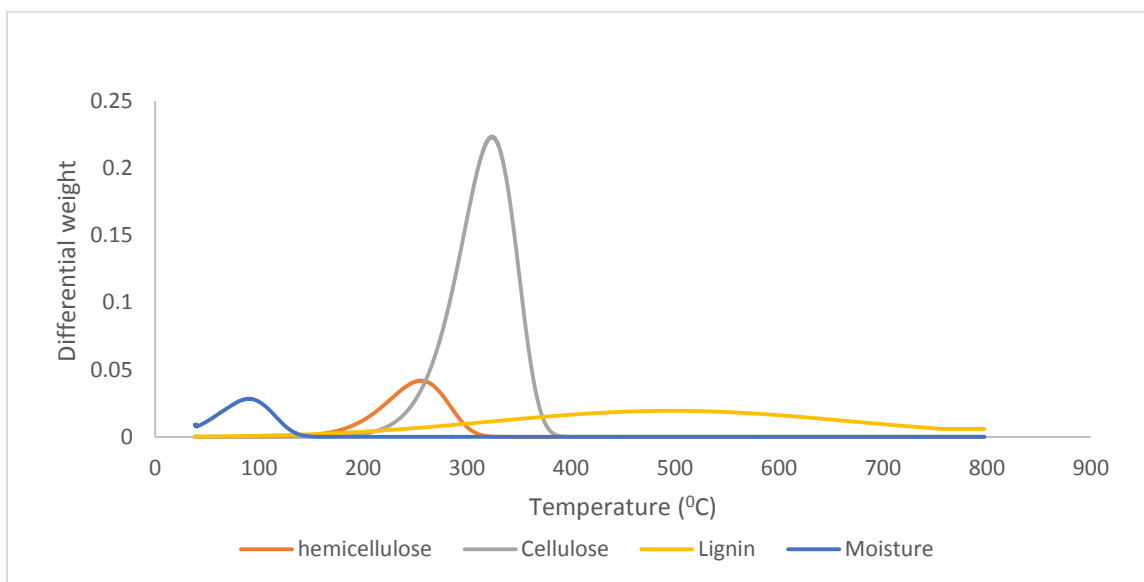


Figure 31 DTG curves of pseudo components obtained from kinetic modelling of pyrolysis

The error associated with the model is shown in table 14. Error mentioned here is objective function (O.F.) shown in equation (7.11) which is summation of square of difference of experimental value and model value. As, modelling of pyrolysis of different heat rates was done separately, errors associated with it is written separately. P5, P20, P50 and P100 is the heat rate associated with pyrolysis process 5 °C/min, 20 °C/min, 50 °C/min and 100 °C/min respectively. Total number of steps in each of the experiment of pyrolysis is different due to different heat rates. Curve fitting percentage was found out using equation (7.12).

Table 14 Errors and curve fitting associated with pyrolysis modelling

	Error	N	$(W_{\max})_{\text{exp}}$	Fit (%)
P5	15.27	3794	9.59	99.34
P20	80.57	3240	10.79	98.54
P50	113.96	2556	10.60	98.01
P100	97.86	2328	10.97	98.13
Total	307.66			

As, discussed by Liu Qian et al., with changes in heating rate it is expected that the apparent activation energy of biomass changes and it increases with the increase in heating rate. On the contrary, here for all four heat rates, only single value of activation energy of a pseudo component is used. So, value of activation energy shown in table 13 is actually average value of activation energy of different heat rates. [60]

Comparison of experimental TG curves and modelling curves of pyrolysis at different heat rates is shown in figure 32.

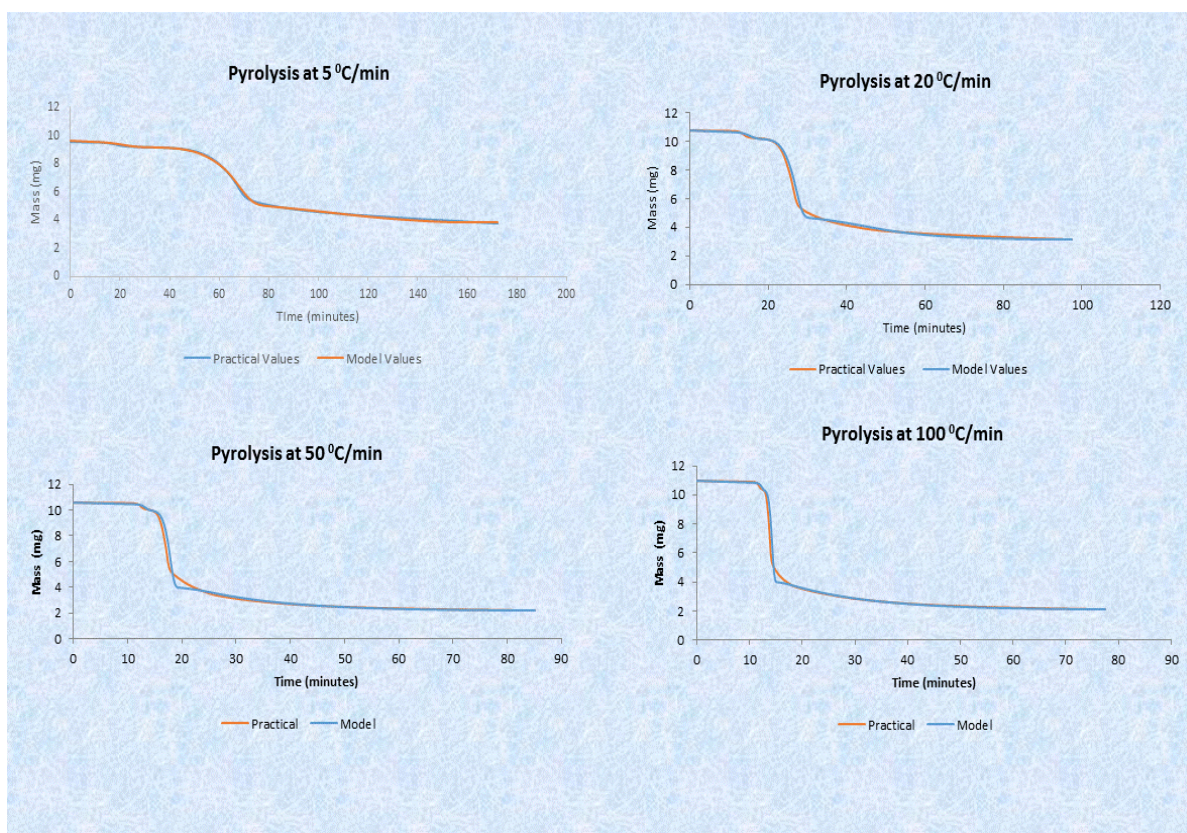


Figure 32 Comparison of TG curves of modelling and experimental values at different heat rates

7.5 Kinetic Model for Combustion

Model

As mentioned earlier, during combustion process first moisture evaporates then vaporization and combustion of volatile matter occurs and then at more elevated temperatures combustion of char occurs and the component of biomass which are associated with volatiles are mainly cellulose and hemicellulose and with char is lignin. This is also discussed by Orfão, J. J. M. in their experiments of biomass combustion that initially combustion of hemicellulose (xylan) starts followed by cellulose and lignin. So, there are three different temperatures at which combustion of these three component will occur. Also, combustion process is quick and it shows a very sharp peak in DTG curve [50, 52].

To get initial data of thermo gravimetric process for modelling, experiments of combustion were done as mentioned in section 6.4 of the report. Experiments were performed at four different heating rates (5, 20, 50 and 100 °C/min) using always the same air flow (50 ml/min) from initial temperature of 40 °C to 800 °C. The details for the experiments are mentioned in table 8.

Kinetic modelling of combustion process is similar to modelling of pyrolysis. All the equations (equations (7.7) to (7.12)) and process mentioned in modelling of pyrolysis are used in the same manner except for equation (7.8). Equation (7.8) has to be modified to account for the influence of oxygen in the combustion process. Equation (7.13) is the modified equation which has an extra component multiplied i.e. partial pressure of oxygen which is constant for all experiments $p_{O_2}=0.21$ atm [61].

$$\frac{dW}{dt} = k(T) * W * p_{O_2} \quad (7.13)$$

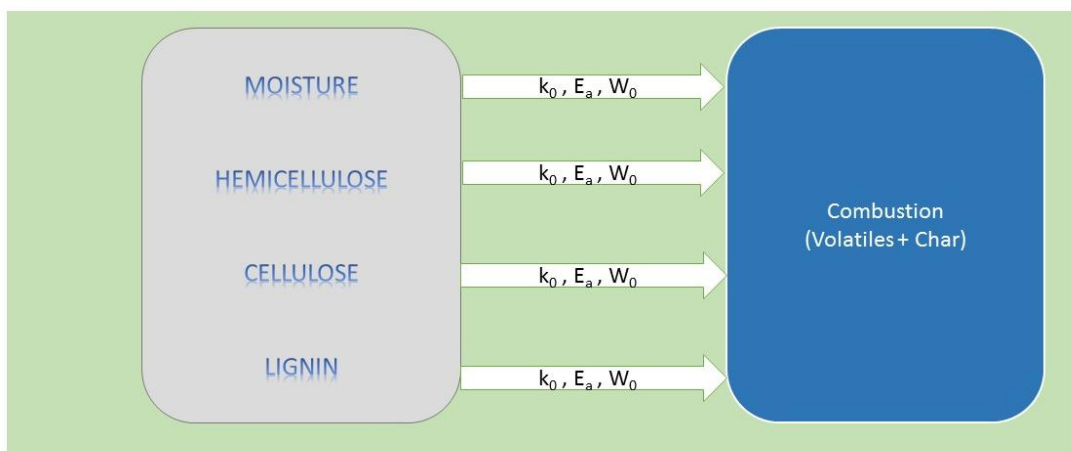


Figure 33 Mechanism of the kinetic modelling of combustion

Whole process of modelling can be explained in figure 33 as shown above. Initially, four pseudo components' (moisture, hemicellulose, cellulose and lignin) rate constant at T_{ref} (k_0), activation energy E_a and initial weight W_0 of each component is assumed. For all the four heat rate variations (5, 20, 50 and 100 °C/min), rate constant at T_{ref} and activation energy of each pseudo component is taken as same.

Results

Composition of four pseudo components estimated from modelling is tabulated in table 15. From the results, amount of hemicellulose and cellulose increases with increase in heat rate while amount of lignin decreases with increase in heat rate. As increase in heat rate volatilizes biomass rapidly, more amount of volatile matter will be generated and combusted than char. When the heat rate is low, generation of char is more. This will result into higher peaks in the char region of combustion than combustion at high heat rates shown in figure 24. This characteristic is explained in section 6.4 of the report.

Dried cattle dung is not homogeneous in nature. Composition of mineral matter varies with batch of production and feedstock given to cattle and its digestion are uncontrollable process. Generally ash content in dried dung varies between 15-30%. [62] Here the batch of production of dung cake is different that justifies varied ash content than it is mentioned in table 5. Moisture content is found out to be almost constant around 5% seems comparable to pyrolysis.

Table 15 Composition of lignocellulosic material in combustion at different heat rates

Composition	Hemicellulose (%)	Cellulose (%)	Lignin (%)	Ash (%)	Moisture (%)
C5	10.34	31.88	28.82	24.11	4.85
C20	10.48	39.37	24.72	20.25	5.17
C50	16.62	44.23	16.51	17.98	4.67
C100	13.60	42.01	17.56	20.84	5.99

Activation energies of pseudo components are shown in table 16. From the experiments of J. J. Orfão of combustion of different components of lignocellulosic biomass it can be deduced that while combusting biomass initially moisture evaporates followed by combustion of hemicellulose, cellulose (volatiles) and lignin (char) structure. [52]

Table 16 Activation energies of pseudo components

	Hemicellulose	Cellulose	Lignin	Moisture
$k(300)$ (1/min)	0.52	0.18	0.01	43.15
E_a (kcal/mol)	20.42	24.69	19.76	9.48

Here, activation energies of all three lignocellulosic pseudo component is in the same range between 20 to 25 kcal/mol. So, $k(300)$ value will decide which component will combust first. Hemicellulose has higher value of $k(300)$ followed by cellulose and lignin. So, as per model, first hemicellulose will burn followed by cellulose and lignin. This can be observed from the differential curves obtained during modelling, shown in figure 34. As observed from figure 34, initially moisture evaporates followed by hemicellulose, cellulose and lignin combustion with cellulose having very sharp peak.

The activation energy for moisture is obtained from modelling is similar to one obtained in modelling of pyrolysis. Theoretical values obtained from modelling is 9.48 kcal/mol which is very near to literature value of 9.67 kcal/mol [59], and also to the value previously obtained in the pyrolysis experiments.

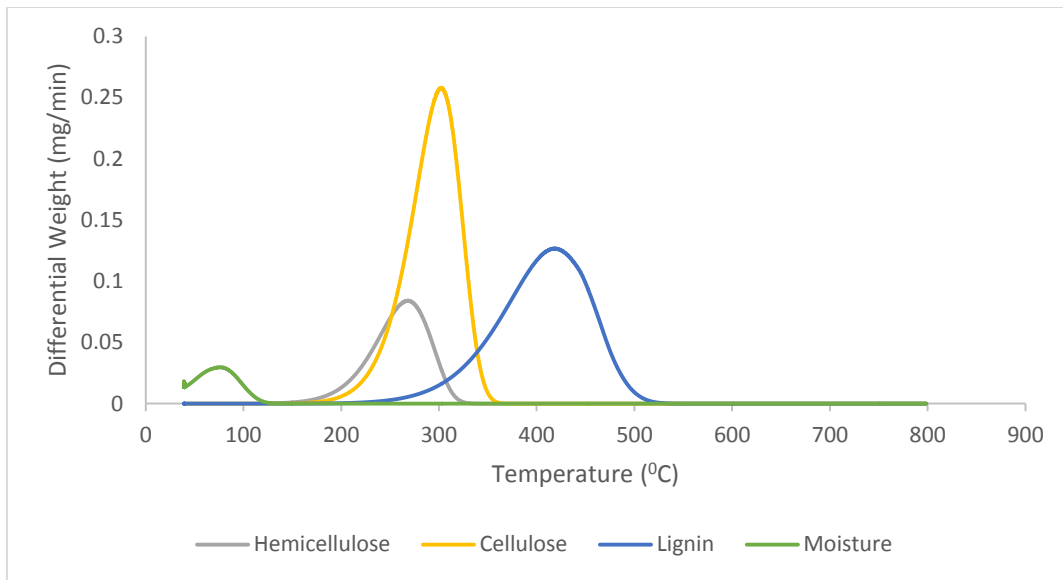


Figure 34 Differential curves of pseudo components obtained from kinetic modelling of combustion

The error associated with modelling is shown in table 17. As, modelling of combustion of different heat rates was done separately but having same values of activation energy and $k(300)$, errors associated with it are written separately. C5, C20, C50 and C100 is the heat rate associated with combustion process 5 °C/min, 20 °C/min, 50 °C/min and 100 °C/min respectively. Total number of steps in each of the experiment of combustion is different due to different heat rates. Curve fitting percentage was found out using equation (7.12).

Table 17 Errors and curve fitting associated with combustion modelling

	Error	N	$(W_{\max})_{\text{exp}}$	Fit (%)
C5	15.27	3794	10.397	99.38975
C20	60.29	2040	10.0472	98.28898
C50	90.41	1656	10.1779	97.70427
C100	63.59	1428	10.4298	97.97666
Total	229.56			

Similar to modelling of pyrolysis, for all four heat rates, only on single value of activation energy for each pseudo component is used for combustion. So, value of the activation energy shown in table 17 is average value of activation energy of different heat rates

Comparison of experimental TG curves and modelling curves of combustion at different heat rates is shown in figure 35.

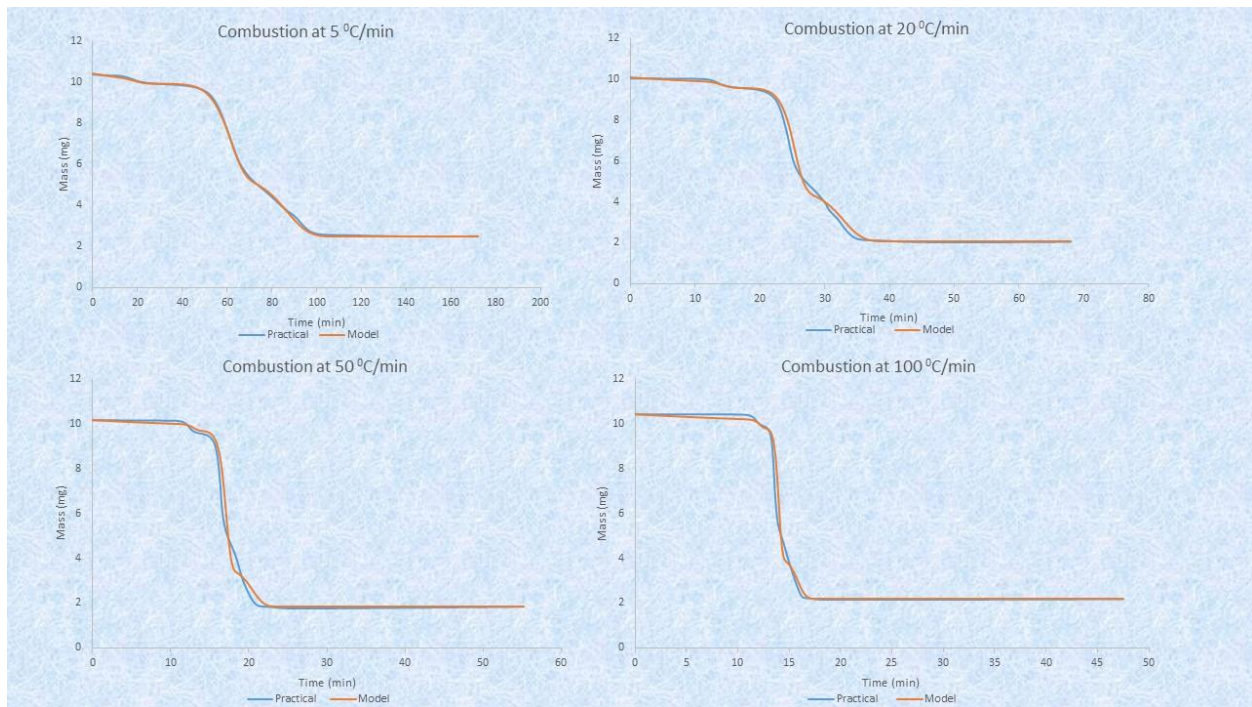


Figure 35 Comparison of TG curves of modelling and experimental values at different heat rates

7.6 Kinetic Model for Partial Oxidation

Thermogravimetric experiments were performed as discussed in section 6.5. For partial combustion, six experiments with same heat rate and different oxygen content are done. Programming for experiment is shown in table 10. For partial oxidation, air quantity is varied from complete combustion (50 ml/min of air) to pyrolysis (no air). Total flow in the furnace is 50 ml/min and it is maintained constant for all the experiments.

Model

Here, main assumption considered during modelling is that partial oxidation is considered as a mixture of pyrolysis and combustion. Three pseudo lignocellulosic components will simultaneously be converted by pyrolysis and by combustion, whereby they will have a fraction of pyrolyzable material and fraction of combustible material. As, discussed by Amutio[50] while modelling it is assumed that pyrolyzable fraction of the pseudo component has same activation energy and $k(300)$ as of pyrolysis process and non pyrolyzable (combustible) fraction has same activation energy and $k(300)$ as of combustion process.

Kinetic modelling of partial oxidation is similar to modelling of pyrolysis and combustion but equations used for it will be modified for partial oxidation. Equation (7.8) is modified to accommodate dual effect of pyrolysis and combustion as below,

$$\frac{dW}{dt} = -k(T)_C * W * r - k(T)_P * W \quad (7.14)$$

Where $k(T)_C$, $k(T)_P$ and r for all pseudo components are computed with help of following equations,

$$k(T)_C = k(300)_C * e^{\frac{(-E_a)_C}{R} \left[\frac{1}{T} - \frac{1}{T_{ref}} \right]} \quad (7.15)$$

$$k(T)_P = k(300)_P * e^{\frac{(-E_a)_P}{R} \left[\frac{1}{T} - \frac{1}{T_{ref}} \right]} \quad (7.16)$$

$$r = \frac{p^{O_2}}{p^{O_2} + k} \quad (7.16)$$

Where, $(E_a)_C$ and $(E_a)_P$ are activation energies associated with combustion and pyrolysis respectively. $T_{ref}=300^\circ\text{C}$ and W is weight of pseudo component and T is temperature at any step of experiment. $k(300)_C$ and $k(300)_P$ are rate constant at reference temperature associated with combustion and pyrolysis respectively. R is gas constant. k is adsorption constant included for Langmuir adsorption as mentioned in

equation (7.5). Rest of the equation i.e. from equation (7.9) to (7.12) and modelling process is similar to modelling of pyrolysis and combustion.

Mechanism for kinetic modelling is shown in figure 36. Two portions pyrolyzable and non pyrolyzable content combined in equation (7.14). As mentioned before, for all pseudo components, value of activation energy E_a and $k(300)$ is taken as same as obtained in pyrolysis and combustion counterpart which is shown in table 18. So, variables left in the process are initial values of pseudo components W_{01} , W_{02} , W_{03} and W_{04} respectively for moisture, hemicellulose, cellulose and lignin and Langmuir adsorption coefficient k .

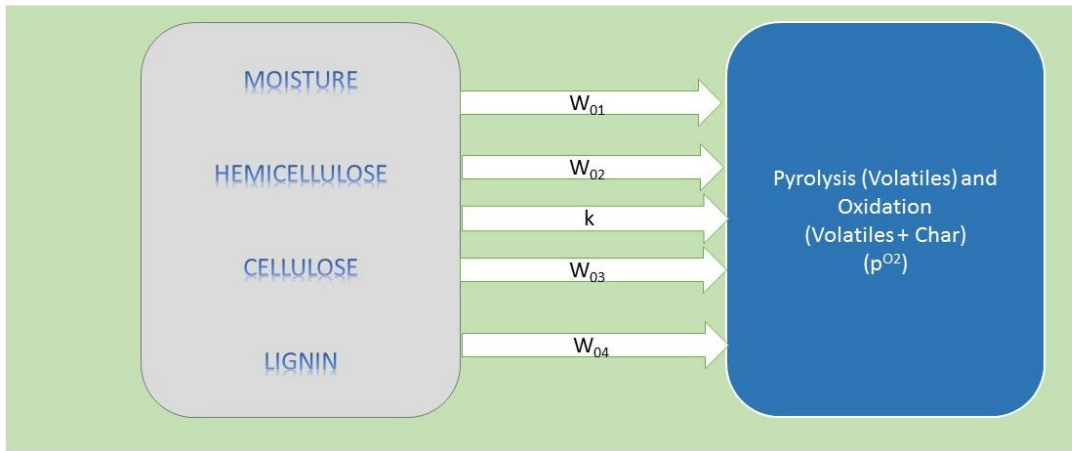


Figure 36 Mechanism of the kinetic modelling of partial oxidation

Moisture evaporation does not have any change due to the partial pressure of oxygen. The only thing that affects evaporation of moisture is temperature. So, values of kinetic parameters of moisture for partial oxidation are taken as same of combustion as it has lower values of error.

Table 18 Values of kinetic parameters of pyrolysis and combustion obtained during modelling

	Pyrolysis				Combustion			
	Hemicellulose	Cellulose	Lignin	Moisture	Hemicellulose	Cellulose	Lignin	Moisture
$k(300)$ (1/min)	0.62	0.073	0.0067	43.14	0.52	0.18	0.01	43.14
E_a (kcal/mol)	18.05	24.98	5.53	9.48	20.43	24.70	19.76	9.49

Results

At higher partial pressure, amount of O₂ is high. So, combustion parameters will dominate the process at higher partial pressure and pyrolysis parameters will dominate at lower partial pressure. Value of k from modelling is found out as 0.3 atm.

Composition of four pseudo components hemicellulose, cellulose, lignin and moisture is mentioned in table 19. Moisture content is ranging between 3.6 to 4.8 %. Whereas, ash content increases with decrease in partial pressure of oxygen. Signifies that lack of oxygen for burning contributes to more char generation. Ash content is highest with no oxygen (pyrolysis). As such, during partial oxidation, there is no correlation between hemicellulose, cellulose and lignin content with variation in partial pressure. Lignin content remained constant in all partial oxidation experiment.

Table 19 Composition of lignocellulosic material in partial oxidation at different heat rates

p _{O2} (atm)	Hemicellulose (%)	Cellulose (%)	Lignin (%)	Ash* (%)	Moisture (%)
0.21	10.24	30.92	30.17	23.87	4.79
0.105	12.38	37.86	30.69	15.18	3.89
0.0525	5.90	40.40	29.51	20.06	4.14
0.021	5.87	30.08	28.93	30.73	4.39
0.0105	7.91	34.55	29.74	23.91	3.88
0	10.91	27.39	18.69	39.37	3.64

*ash may contain char.

As programming (cycle) used for all partial oxidation TG experiments is same, number of steps N is same for all the experiments. Error associated with modelling is shown in table 20. As, modelling of partial oxidation at different oxygen content was done separately but having same values of activation energy and k(300), errors associated with it is written separately. Six different partial pressure of oxygen with same heat rate 5 °C/min was used. Curve fitting percentage was found out using equation (7.12).

Table 20 Errors and curve fitting associated with combustion modelling

p _{O2} (atm)	Error	N	(W _{exp}) _{max}	Fit (%)
0.21	87.62	3794	10.40	98.54
0.105	143.63	3794	10.43	98.13
0.0525	145.53	3794	10.03	98.05
0.021	161.73	3794	10.53	98.04
0.0105	192.81	3794	10.04	97.75
0	45.17	3794	9.59	98.86
Total	776.49			

Comparison of experimental TG curves and modelling curves of partial oxidation at different partial pressure of oxygen is shown in figure 37. Errors associated with modelling is higher for $p^{O_2} = 0.105, 0.0525, 0.021, 0.0105$ atm.

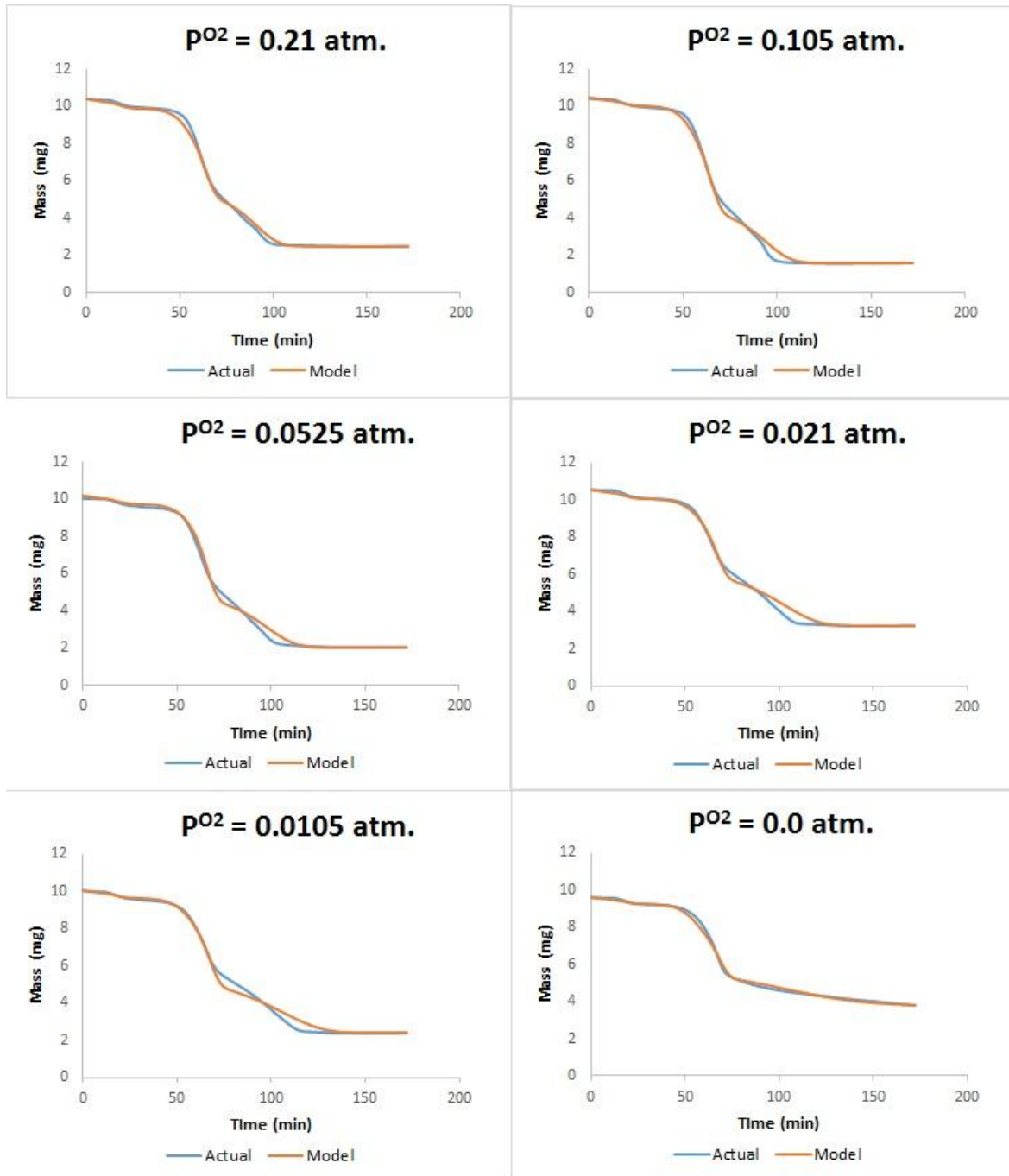


Figure 37 Comparison of TG curves of modelling and experimental values at different heat rates

As it can be seen the results are quite satisfactory for the extreme cases, pyrolysis or combustion in air, which is understandable as we have used the parameters derived for these conditions in the previous experiments, but the model still requires some refining to describe the intermediate conditions.

The development of a model that can be used across a large range of experimental conditions is important if we wish to model and design an actual gasifier to be able to describe the reaction kinetics in the various sections of the gasifier, where different conditions prevail.

Chapter 8 Analysis of Ash

8.1 Introduction

Cattle manure is the oldest fertilizer that human being is still using for farming. But now, use of cattle manure in farms is a popular practice in only few rural areas. This type of manure is not as rich in nitrogen as many other type of fertilizer, also the high ammonia levels present can burn plants when the fresh manure is directly applied. For this reason, cow manure is usually aged or composted prior to its use as fertilizer. Composting manure eliminates harmful ammonia, pathogens and weed seeds, although with an environmental cost. Cattle manure is basically made up of digested grass and grain. Cow dung is high in organic materials and rich in nutrients. It contains about 3% nitrogen (N), 2% phosphorus (P) , and 1% potassium (K) (3-2-1 NPK). [62]

8.2 Importance of N-P-K in plant growth

An ideal fertilizer should consist of three basic element of plant growth nitrogen, phosphorus, and potassium. Nitrogen is primarily responsible for vegetative growth. Nitrogen assimilation into amino acids is the building block for protein in the plant. It is a component of chlorophyll and is required for several enzyme reactions. Phosphorus is a major component in plant DNA and RNA. Phosphorus is also critical in root development, crop maturity and seed production. The role of potassium in the plant is indirect, meaning that it does not make up any plant part. Potassium is required for the activation of over 80 enzymes throughout the plant. It's important for a plant's ability to withstand extreme cold and hot temperatures, drought and pests. Potassium increases water use efficiency and transforms sugars to starch in the grain-filling process. Because of this reasons, most of the fertilizers contains N, P, K elements. [63]

8.3 Ash composition and usage as fertilizer

Here, cattle manure is characterized for usage in thermochemical processes. This process would allow the recovery of energy from the manure while leaving the inorganic components behind for usage as fertilizers. The only mass left in this process, after the thermochemical energy conversion, is ash. As discussed earlier that manure contains N-P-K, but during thermochemical processes, nitrogen is lost to atmosphere. For direct usage or for recovery of P and K for fertilizer, study on ash content has to be done. In table 20, composition of feedlot manure ash studied by Sweeten, John M., et al. is shown [64]. As we can see, ash contains around 3% of P_2O_5 and 6.4% of K_2O , both are water soluble. It also contains other useful plant requirements like CaO , MgO etc. In, next section analysis of Phosphorus and Potassium composition of dried cattle dung is discussed.

Table 21 Analysis of cattle manure ash [64]

Component	Wt(% ash)
SO₃	2.80
Cl	3.80
P₂O₅	3.00
SiO₂	53.49
Fe₂O₃	1.70
Al₂O₃	7.80
CaO	13.90
MgO	3.70
Na₂O	2.00
K₂O	6.40
TiO₂	0.33

8.4 P and K analysis

Methodology

Ash used in analysis was collected from combustion of feedlot manure. Approximately 40 mg of ash was used in the analysis. The method used for analysis is inductively coupled plasma atomic emission spectroscopy (ICP-AES), also referred to as inductively coupled plasma optical emission spectrometry (ICP-OES), a trace metal element analysis method. Trace metal analysis shows amount of metal present in the sample.

Result

Result of the analysis is shown in table 22. Result is presented as percentage of P and K in total ash content. Phosphorus as metal element is 3.1% and Potassium is 6.5%.

Table 22 Elemental analysis of Phosphorus and Potassium

Element	Amount (%)
Phosphorus	3.1
Potassium	6.5

This indicates that the ash resulting from the pyrolysis or combustion processes still can be used as phosphorous and potassium sources in agriculture.

8.5 Further Application

From the results, there can be three possible ways to utilize dung ash for further usage

- This dried dung ash can be directly utilized as fertilizer for legumes species of crops. Legumes' roots contains bacteria that produce the nitrogen required for the plant. As cattle dung ash from thermochemical processes does not contain nitrogen, this application can be the best suited method [66].
- Dung ash does not contain nitrogen. To supplement nitrogen, manure urine can be used as urine contains nitrogen. By this manner, it can be used as a normal fertilizer and can be tested further. Only problem with this method is to control pH of the soil as mixture of both ash and urine can be more acidic and that may not be suitable for certain plants. [67]
- Recovery of Phosphorus and Potassium can also be possible. This recovery can be done by chemical extraction, bleaching, supercritical water extractions etc., [68] Recovered P and K can further be utilized to make synthetic fertilizers or can be used for other chemical applications.

Ash contains various acidic and basic oxides which react with water and makes acids and bases. So, before any application pH of ash in water has to be checked.

Conclusion

Thermal Analysis

1) Pyrolysis

From TG curves of pyrolysis of dried cattle dung, three different types of reactions were observed due to three different slopes in TG curve i.e. i) Evaporation of moisture (from 40 °C to 200 °C) ii) decomposition and evaporation of pyrolyzable matter from cellulose and hemicellulose (from 200 °C to 400 °C) and iii) decomposition and evaporation of pyrolyzable matter from lignin (from 400 °C to 800 °C).

The higher the heating rate during the pyrolysis process, the lower the char content and higher volatile matter is produced and vice versa. As the heating rate increases, heat release rate from fuel also increases because of scission, dehydration, disproportionation and decarboxylation reactions of polysaccharides compounds present in hemicellulose and cellulose. Ignition temperature of char obtained from pyrolysis of dung cake is about 300 °C and peak temperature is around 420 °C.

2) Combustion

From DTG curves of combustion of dried cattle dung, three different types of reactions were observed due to three different peaks in DTG curve i.e. i) Evaporation of moisture (from 40 °C to 180 °C) ii) combustion of volatile matter and char reduction (from 180 °C to 400 °C) and iii) combustion of char (from 400 °C to 500 °C).

As heat rate increases, ignition temperature, peak temperature and peak combustion rate increase and because of this shift or delay, combustion of char also falls in that regime of temperature. Thus, combustion of char is not well observed during the experiment at 100 °C/min.

3) Partial Oxidation

As oxygen supplied to biomass decreases during different oxidation experiments, ignition temperature, peak temperature increases and peak combustion rate decreases because lack of oxygen causes ignition delay and delays combustion process.

When partial pressure of oxygen decreases, char combustion rate decreases and maximum char combustion temperature increases.

As oxygen content decreases, amount of heat released from sample decreases. This can be explained by Lower oxygen supply that causes production of CO instead of CO₂ which has a lower exothermicity.

Kinetic Modelling

Comparison of activation energy, rate constants at reference temperature and error associated with modelling is shown in table 23. The third peak of char combustion during combustion of dried dung explains higher value of activation energy E_a and rate constant at reference temperature $k(300)$ compared to that obtained by pyrolysis. Activation energy of moisture in both cases are the same. The error associated with modelling of pyrolysis is higher compared to modelling of combustion. Value of Langmuir constant (k) obtained through modelling of partial oxidation process is 0.3 atm.

Table 23 Comparison of Kinetic parameters of pyrolysis and combustion

Process	Pseudo Component	k(300) (1/min)	Ea (kcal/mol)
Pyrolysis	Hemicellulose	0.62	18.05
	Cellulose	0.073	24.98
	Lignin	0.0067	5.53
	Moisture	22.48	9.47
Combustion	Hemicellulose	0.52	20.43
	Cellulose	0.18	24.7
	Lignin	0.01	19.76
	Moisture	43.14	9.49

Ash Analysis

Values of phosphorus and potassium obtained from elemental analysis of ash are 3.1 % and 6.5 % which is very significant for its usage as fertilizer. This ash can be used as direct fertilizer to legumes plant, to be made as perfect fertilizer by mixing it with nitrogen containing solutions like animal urine or recovery of phosphorus and potassium from ash through various processes and utilize it to make synthetic fertilizer.

Future Proposal

Although thesis is intended towards design of a gasifier, due to time limitation kinetic analysis of gasification parameters and ash analysis can be done. The future system for energy generation and ash utilization is shown in figure 38. As we know that as received cattle dung contains high amount of moisture (20-60 %) and if it is used directly into gasifier, it will decrease yield. So, drying system is necessary. Tropical countries like India and Brazil (together contains half of world's cattle inventory) have throughout the year high temperatures and comparative higher sunshine hours. So, solar assisted drying system proposed by Panchal H.N. et al. [70] can also be used to make system more efficient. Dried cattle dung (moisture content 5 to 8%) can be used in gasifier system to produce syngas. Syngas can further be utilized for electricity production through coupled I.C. engine or to produce other chemical synthesis fuels. Ash left in the bottom of gasifier can be further used for fertilizer usage or metal recovery.

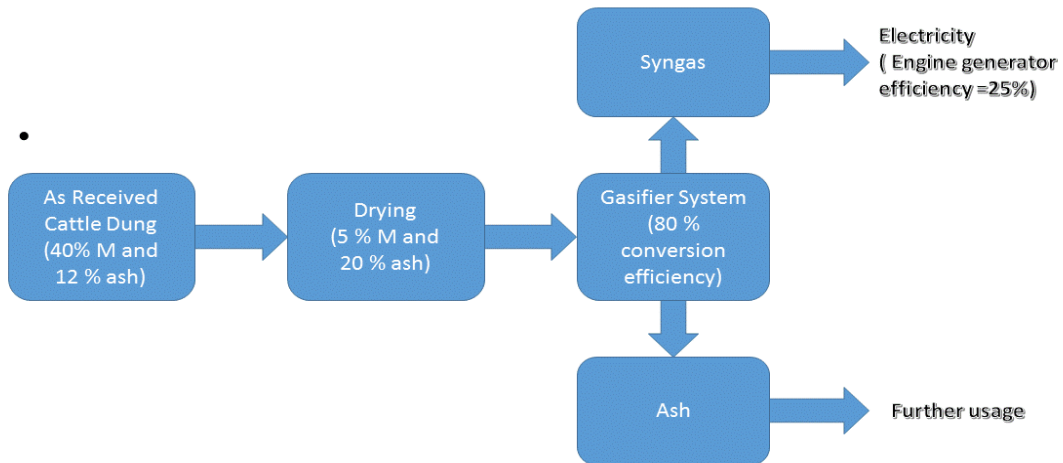


Figure 38 Proposed system for future work

For viability of the system, energy calculations on a primary basis is done. For that there are some assumption is done which are as follows:

- As received moisture content is 40 % and ash content is 12% and after drying moisture is 5 % and ash is 20%.
- Gasifier system efficiency is 80% and engine generator efficiency is 25 %.
- One cow produces 25 kg of dung. [69]

For drying system, to reduce moisture content from 40 % to 5 % for 1 kg of as received feedstock, 10 % of total energy of as received feedstock (LCV = 9360 kJ/kg as received) is used. Considering assumed efficiencies of gasifier system and engine generator system and total dung produced by a cow, one cow can produce 12 units of electricity (42.29 MJ) per day.

References

1. Hall, D.O., Rosillo-Calle, F., Woods, J., & Williams, R.H. (1993). Biomass for energy: Supply prospects. United States: Island Press, Washington, DC (United States).
2. Klass, D. L. (1998). Biomass for renewable energy, fuels, and chemicals. Academic press.
3. Sims, R. E., Hastings, A., Schlamadinger, B., Taylor, G., & Smith, P. (2006). Energy crops: current status and future prospects. *Global Change Biology*, 12(11), 2054-2076.
4. Basu, P. (2010). Biomass gasification and pyrolysis: practical design and theory. Academic press.
5. Diebold, J. P., & Bridgwater, A. V. (1997). Overview of fast pyrolysis of biomass for the production of liquid fuels. In *Developments in thermochemical biomass conversion* (pp. 5-23). Springer Netherlands.
6. Pimchuai, A., Dutta, A., & Basu, P. (2010). Torrefaction of agriculture residue to enhance combustible properties†. *Energy & Fuels*, 24(9), 4638-4645.
7. Jahirul, M. I., Rasul, M. G., Chowdhury, A. A., & Ashwath, N. (2012). Biofuels production through biomass pyrolysis—a technological review. *Energies*, 5(12), 4952-5001.
8. Fisher, T., Hajaligol, M., Waymack, B., & Kellogg, D. (2002). Pyrolysis behavior and kinetics of biomass derived materials. *Journal of analytical and applied pyrolysis*, 62(2), 331-349.
9. Lanzetta, M., & Di Blasi, C. (1998). Pyrolysis kinetics of wheat and corn straw. *Journal of Analytical and Applied Pyrolysis*, 44(2), 181-192.
10. Venderbosch, R. H., & Prins, W. (2010). Fast pyrolysis technology development. *Biofuels, bioproducts and biorefining*, 4(2), 178-208.
11. Balat, M., Balat, M., Kirtay, E., & Balat, H. (2009). Main routes for the thermo-conversion of biomass into fuels and chemicals. Part 1: Pyrolysis systems. *Energy Conversion and Management*, 50(12), 3147-3157.
12. Bridgwater, T. (2007). Pyrolysis of Biomass. IEA Bioenergy: Task 34. Bioenergy Research Group, Aston University, Birmingham, UK.
13. Bridgwater, A. V., Czernik, S., & Piskorz, J. (2001). An overview of fast pyrolysis. *Progress in thermochemical biomass conversion*, 977-997.
14. Hilal DemirbaŞ, A. (2005). Yields and heating values of liquids and chars from spruce trunk bark pyrolysis. *Energy sources*, 27(14), 1367-1373.
15. Demirbas, A., & Arin, G. (2002). An overview of biomass pyrolysis. *Energy sources*, 24(5), 471-482.
16. Brammer, J. G., Lauer, M., & Bridgwater, A. V. (2006). Opportunities for biomass-derived “bio-oil” in European heat and power markets. *Energy policy*, 34(17), 2871-2880.
17. Chiaramonti, D., Oasmaa, A., & Solantausta, Y. (2007). Power generation using fast pyrolysis liquids from biomass. *Renewable and sustainable energy reviews*, 11(6), 1056-1086.
18. L  d  , J., Diebold, J. P., Peacocke, G. V. C., Piskorz, J., Bridgwater, A. V., Czernik, S., ... & Radlein, D. (1999). *Fast Pyrolysis of Biomass: A Handbook*.

19. Aguado, R., Olazar, M., Gaisán, B., Prieto, R., & Bilbao, J. (2002). Kinetic study of polyolefin pyrolysis in a conical spouted bed reactor. *Industrial & engineering chemistry research*, 41(18), 4559-4566.
20. Cornelissen, T., Yperman, J., Reggers, G., Schreurs, S., & Carleer, R. (2008). Flash co-pyrolysis of biomass with polylactic acid. Part 1: Influence on bio-oil yield and heating value. *Fuel*, 87(7), 1031-1041.
21. Rajvanshi, A. K. (1986). Biomass gasification. *Alternative energy in agriculture*, 2(4), 82-102.
22. Abdollahi-Neisiani, M., Laviolette, J. P., Jafari, R., & Chaouki, J. (2013). Biomass Pretreatments for Biorefinery Applications: Gasification. In *Pretreatment Techniques for Biofuels and Biorefineries* (pp. 197-227). Springer Berlin Heidelberg.
23. Yin, C. Y. (2011). Prediction of higher heating values of biomass from proximate and ultimate analyses. *Fuel*, 90(3), 1128-1132.
24. Dasappa, S. (2014). Thermochemical Conversion of Biomass. *Transformation of Biomass: Theory to Practice*, 133-157.
25. Pachauri, R. K., Allen, M. R., Barros, V. R., Broome, J., Cramer, W., Christ, R., Dubash, N. K. (2014). Climate change 2014: synthesis Report. Contribution of working groups I, II and III to the fifth assessment report of the intergovernmental panel on climate change (p. 151). IPCC.
26. Tubiello, F. N., Salvatore, M., Córdor Golec, R. D., Ferrara, A., Rossi, S., Biancalani, R., Flammini, A. (2014). Agriculture, forestry and other land use emissions by sources and removals by sinks. Statistics Division, Food and Agriculture Organization, Rome.
27. Holm-Nielsen, J. B., Al Seadi, T., & Oleskowicz-Popiel, P. (2009). The future of anaerobic digestion and biogas utilization. *Bioresource technology*, 100(22), 5478-5484.
28. Demirel, B., & Scherer, P. (2008). The roles of acetotrophic and hydrogenotrophic methanogens during anaerobic conversion of biomass to methane: a review. *Reviews in Environmental Science and Bio/Technology*, 7(2), 173-190.
29. Smith, K. R., Samet, J. M., Romieu, I., & Bruce, N. (2000). Indoor air pollution in developing countries and acute lower respiratory infections in children. *Thorax*, 55(6), 518-532.
30. Kankaria, A., Nongkynrih, B., & Gupta, S. K. (2014). Indoor air pollution in India: Implications on health and its control. *Indian journal of community medicine: official publication of Indian Association of Preventive & Social Medicine*, 39(4), 203.
31. Raiyani, C. V., Jani, J. P., Desai, N. M., Shah, S. H., Shah, P. G., & Kashyap, S. K. (1993). Assessment of indoor exposure to polycyclic aromatic hydrocarbons for urban poor using various types of cooking fuels. *Bulletin of environmental contamination and toxicology*, 50(5), 757-763.
32. Kandpal, J. B., Maheshwari, R. C., & Kandpal, T. C. (1995). Indoor air pollution from combustion of wood and dung cake and their processed fuels in domestic cookstoves. *Energy conversion and management*, 36(11), 1073-1079.
33. Wright, M. R. (2005). *Introduction to Chemical Kinetics*. John Wiley & Sons.

34. Skinner, G. (2012). Introduction to chemical kinetics. Elsevier.
35. Khawam, A., & Flanagan, D. R. (2006). Solid-state kinetic models: basics and mathematical fundamentals. *The journal of physical chemistry B*, 110(35), 17315-17328.
36. Bhatia, S. K., & Perlmutter, D. D. (1980). A random pore model for fluid-solid reactions: I. Isothermal, kinetic control. *AIChE Journal*, 26(3), 379-386.
37. Karathanasis, A. D., & Harris, W. G. (1994). Quantitative thermal analysis of soil materials. *Quantitative methods in soil mineralogy*, (quantitativemet), 360-411.
38. Plante, A. F., Fernández, J. M., & Leifeld, J. (2009). Application of thermal analysis techniques in soil science. *Geoderma*, 153(1), 1-10.
39. Crewe, R. J., Staggs, J. E. J., & Williams, P. T. (2007). Drag-induced apparent mass gain in thermogravimetry. *Polymer Degradation and Stability*, 92(11), 2070-2075.
40. Doyle, C. D. (1961). Kinetic analysis of thermogravimetric data. *Journal of applied polymer science*, 5(15), 285-292.
41. Coats, A. W., & Redfern, J. P. (1963). Thermogravimetric analysis. A review. *Analyst*, 88(1053), 906-924.
42. El-Sayed, S. A., & Mostafa, M. E. (2015). Kinetic parameters determination of biomass pyrolysis fuels using TGA and DTA techniques. *Waste and Biomass Valorization*, 6(3), 401-415.
43. Channiwala, S. A., & Parikh, P. P. (2002). A unified correlation for estimating HHV of solid, liquid and gaseous fuels. *Fuel*, 81(8), 1051-1063.
44. Mansaray, K. G., & Ghaly, A. E. (1999). Determination of kinetic parameters of rice husks in oxygen using thermogravimetric analysis. *Biomass and Bioenergy*, 17(1), 19-31.
45. Yang, H., Yan, R., Chen, H., Lee, D. H., & Zheng, C. (2007). Characteristics of hemicellulose, cellulose and lignin pyrolysis. *Fuel*, 86(12), 1781-1788.
46. Katyal, S., Thambimuthu, K., & Valix, M. (2003). Carbonisation of bagasse in a fixed bed reactor: influence of process variables on char yield and characteristics. *Renewable Energy*, 28(5), 713-725.
47. Shafizadeh, F. (1982). Introduction to pyrolysis of biomass. *Journal of Analytical and Applied Pyrolysis*, 3(4), 283-305.
48. Demirbas, A. (2004). Combustion characteristics of different biomass fuels. *Progress in energy and combustion science*, 30(2), 219-230.
49. Haykırı-Açma, H. (2003). Combustion characteristics of different biomass materials. *Energy Conversion and Management*, 44(1), 155-162.
50. Amutio, M., Lopez, G., Aguado, R., Artetxe, M., Bilbao, J., & Olazar, M. (2012). Kinetic study of lignocellulosic biomass oxidative pyrolysis. *Fuel*, 95, 305-311.
51. Stiller, A. H., Dadyburjor, D. B., Wann, J. P., Tian, D., & Zondlo, J. W. (1996). Co-processing of agricultural and biomass waste with coal. *Fuel processing technology*, 49(1), 167-175.

52. Orfao, J. J. M., Antunes, F. J. A., & Figueiredo, J. L. (1999). Pyrolysis kinetics of lignocellulosic materials—three independent reactions model. *Fuel*, 78(3), 349-358.
53. Galwey, A. K., & Brown, M. E. (2002). Application of the Arrhenius equation to solid state kinetics: can this be justified?. *Thermochimica Acta*, 386(1), 91-98.
54. Senneca, O., Chirone, R., & Salatino, P. (2002). A thermogravimetric study of nonfossil solid fuels. 2. Oxidative pyrolysis and char combustion. *Energy & Fuels*, 16(3), 661-668.
55. Steinfeld, J. I., Francisco, J. S., & Hase, W. L. (1989). *Chemical kinetics and dynamics* (Vol. 3). Englewood Cliffs (New Jersey): Prentice Hall.
56. Langmuir, I. (1918). The adsorption of gases on plane surfaces of glass, mica and platinum. *Journal of the American Chemical society*, 40(9), 1361-1403.
57. Redlich, O. J. D. L., & Peterson, D. L. (1959). A useful adsorption isotherm. *Journal of Physical Chemistry*, 63(6), 1024-1024.
58. Tran, K. Q., Bach, Q. V., Trinh, T. T., & Seisenbaeva, G. (2014). Non-isothermal pyrolysis of torrefied stump—a comparative kinetic evaluation. *Applied Energy*, 136, 759-766.
59. Franks, F. (2000). *Water: a matrix of life* (Vol. 21). Royal Society of Chemistry.
60. Liu, Q., Wang, S., Zheng, Y., Luo, Z., & Cen, K. (2008). Mechanism study of wood lignin pyrolysis by using TG–FTIR analysis. *Journal of Analytical and Applied Pyrolysis*, 82(1), 170-177.
61. Senneca, O. (2007). Kinetics of pyrolysis, combustion and gasification of three biomass fuels. *Fuel Processing Technology*, 88(1), 87-97.
62. Kirchmann, H., & Witter, E. (1992). Composition of fresh, aerobic and anaerobic farm animal dungs. *Bioresource technology*, 40(2), 137-142.
63. Ellis, B. W., Bradley, F. M., & Atthowe, H. (Eds.). (1996). *The organic gardener's handbook of natural insect and disease control: A complete problem-solving guide to keeping your garden and yard healthy without chemicals*. Rodale.
64. Mäder, P., Fliessbach, A., Dubois, D., Gunst, L., Fried, P., & Niggli, U. (2002). Soil fertility and biodiversity in organic farming. *Science*, 296(5573), 1694-1697.
65. Sweeten, J. M., Korenberg, J., LePori, W. A., Annamalai, K., & Parnell, C. B. (1986). Combustion of cattle feedlot manure for energy production. *Energy in agriculture*, 5(1), 55-72.
66. Ghosh, P. K., Bandyopadhyay, K. K., Manna, M. C., Mandal, K. G., Misra, A. K., & Hati, K. M. (2004). Comparative effectiveness of cattle manure, poultry manure, phosphocompost and fertilizer-NPK on three cropping systems in vertisols of semi-arid tropics. II. Dry matter yield, nodulation, chlorophyll content and enzyme activity. *Bioresource technology*, 95(1), 85-93.
67. Pradhan, S. K., Holopainen, J. K., & Heinonen-Tanski, H. (2009). Stored human urine supplemented with wood ash as fertilizer in tomato (*Solanum lycopersicum*) cultivation and its impacts on fruit yield and quality. *Journal of agricultural and food chemistry*, 57(16), 7612-7617.
68. Tan, Z., & Lagerkvist, A. (2011). Phosphorus recovery from the biomass ash: A review. *Renewable and Sustainable Energy Reviews*, 15(8), 3588-3602.

69. Foreign Agricultural Service. 2016. Livestock and Poultry-World Markets and Trade. US Department of Agriculture, Washington, D.C.
70. Panchal, H. N., Doshi, M., Chavda, P., & Goswami, R. (2010). Effect of Cow dung cakes inside basin on heat transfer coefficients and productivity of single basin single slope solar still. International Journal of Applied Engineering Research, 1(4), 675.